



INEEL/EXT-98-01178

Rev. 1

September 1999

# **SCDAP/RELAP5 Modeling of Movement of Melted Material Through Porous Debris in Lower Head**

*L. J. Siefken*

# **SCDAP/RELAP5 Modeling of Movement of Melted Material Through Porous Debris in Lower Head**

**L. J. Siefken**

**Published September 1999**

**Idaho National Engineering and Environmental Laboratory  
Lockheed Martin Idaho Technologies Company  
Idaho Falls, Idaho 83415**

**Prepared for  
Division of Systems Technology  
Office of Nuclear Regulatory Research  
U.S. Nuclear Regulatory Commission  
Washington, DC 20555-0001  
NRC Job Code W6095**

## **ABSTRACT**

The COUPLE model in SCDAP/RELAP5 calculates the heatup of the lower head of a reactor vessel due to contact with core material that has slumped to the lower head during a severe accident in a Light Water Reactor. The COUPLE model calculates the transport of heat by conduction, convection and radiation through the core debris in the lower head and the transport of heat from the core debris to the lower head. Currently, the COUPLE model does not have the capability to model the movement of liquefied core plate material that slumps onto a porous debris bed in the lower head. In order to advance beyond the assumption that liquefied material always remains on top of the porous debris, designs are developed for calculations of the movement of liquefied core plate material through the interstices in a matrix of porous ceramic material. Correlations are identified for calculating the permeability of the porous debris and for calculating the rate of flow of liquefied material through the interstices in the debris bed. Equations are defined for calculating the effect on the temperature distribution in the debris bed of heat transported by moving material and for changes in effective thermal conductivity and heat capacity due to the movement of material. The models are applicable to core plates composed of stainless steel and porous debris beds composed of  $\text{UO}_2$  and  $\text{ZrO}_2$  particles. The implementation of these models is expected to improve the calculation of the material distribution and temperature distribution of debris in the lower head for cases in which the debris is porous and liquefied core plate material is present within the porous debris. This report is a revision of the report with the identifier of INEEL/EXT-98-01178, entitled "SCDAP/RELAP5 Modeling of Movement of Melted Material Through Porous Debris in Lower Head."

# CONTENTS

Abstract.....	v
1. Introduction .....	1
2. Models for Movement of Liquefied Material in Porous Debris .....	3
3. Effects of Liquefied Material Movement on Debris Bed Heat Transfer.....	6
4. Boundary Conditions for Case of Core Plate Melting above Debris Bed .....	10
5. Numerical Solution.....	11
6. Implementation into COUPLE Model.....	19
7. Testing and Assessment of Implemented Models .....	23
8. Summary.....	23
9. References .....	25

# FIGURES

Figure 1-1. Schematic of system represented by COUPLE model (particle size of debris greatly exaggerated). .....	1
Figure 1-2. Previous modeling of liquefied material within porous debris bed. ....	2
Figure 1-3. Extension in modeling of liquefied material within porous debris bed. ....	2
Figure 4-1. Schematic of material movement occurring when core plate melts and lower head supports ceramic porous debris. ....	10
Figure 7-1. Description of test problem number 1. ....	24

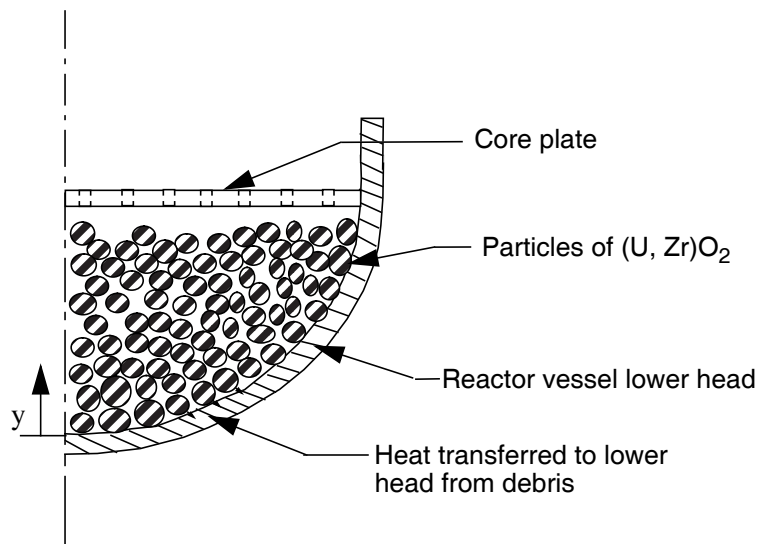
# TABLES

Table 5-1. Characteristics and properties for debris and melted stainless steel for scoping calculations.....	17
Table 5-2. Values of coefficients in Equation (5-12) for two representative cases .....	18
Table 5-3. Superficial velocities for two representative cases .....	18
Table 6-1. Variables added to COUPLE data base for modeling of flow of liquefied material within porous debris bed. ....	20
Table 6-2. User-defined variables added to data base for modeling of flow of liquefied material within porous debris bed. ....	21
Table 6-3. Extensions to existing COUPLE subroutines for modeling flow of liquefied material within porous debris bed. ....	22
Table 7-1. Matrix of test problems for assessing models of liquefied material moving through porous debris bed. ....	23

# 1. Introduction

In the event of a severe accident in a Light Water Reactor (LWR), particles of a ceramic mixture of  $\text{UO}_2$  and  $\text{ZrO}_2$  may stack in the lower head of the reactor vessel and form a porous debris bed. The context of the porous debris bed is shown in Figure 1-1. The slumping of jets of a mixture of molten  $(\text{U,Zr})\text{O}_2$  into a pool of water in the lower head is an example of a reactor core degradation event that may occur during a severe accident and result in the configuration of material shown in Figure 1-1. If the severe accident is not terminated, then eventually the core plate may melt and slump onto the top of the bed of ceramic particles. The core plate is generally composed of stainless steel and thus melts at a much lower temperature than the particles of  $(\text{U, Zr})\text{O}_2$  (1700 K versus ~3000 K). The subsequent heatup of the debris bed and lower head is a function of the extent to which the melted core plate permeates into the bed of  $(\text{U, Zr})\text{O}_2$  particles. This report describes a model for calculating the permeation of the melted core plate material into the porous debris bed and describes the implementation of this model into the existing model in the SCDAP/RELAP5 code<sup>1</sup> for calculating the heatup of the debris bed and lower head supporting the debris bed.

The COUPLE model in SCDAP/RELAP5 calculates the heatup of the lower head and the debris that it supports. The system that the COUPLE model is designed to analyze is shown in Figure 1-1. Previously



**Figure 1-1.** Schematic of system represented by COUPLE model (particle size of debris greatly exaggerated).

the COUPLE model could not calculate the movement of melted material. A schematic of the previous modeling capability with respect to melted material is shown in Figure 1-2. The schematic of modeling capability added to the COUPLE model is shown in Figure 1-3.

This report is organized as follows. Section 2 describes the models applied to calculate the movement of liquefied core plate material through the interstices in a matrix of porous  $(\text{U, Zr})\text{O}_2$  debris. Section 3 describes the effect of liquefied material movement on debris bed heat transfer. Section 4 describes the interface of the COUPLE model for the movement of liquefied material with models that

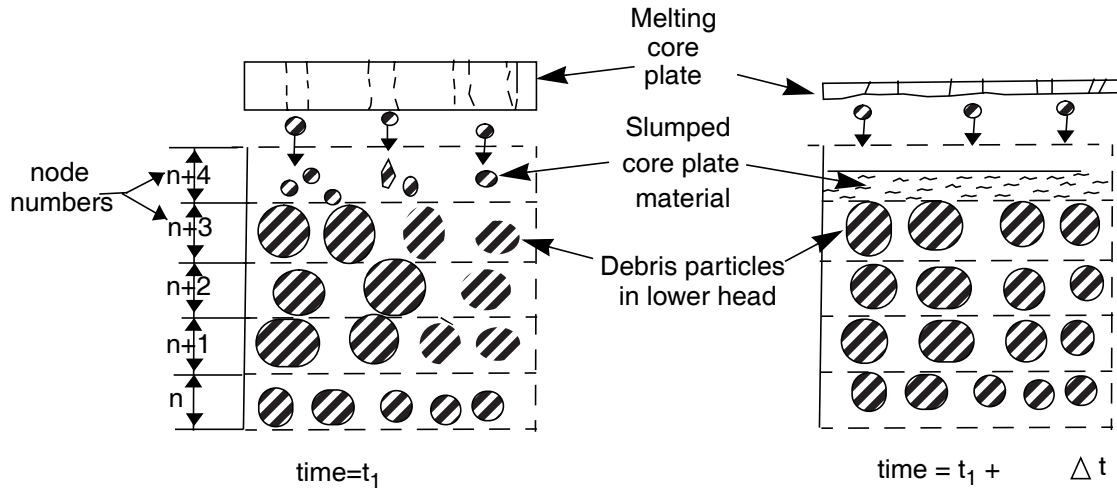


**Figure 1-2.** Previous modeling of liquefied material within porous debris bed.

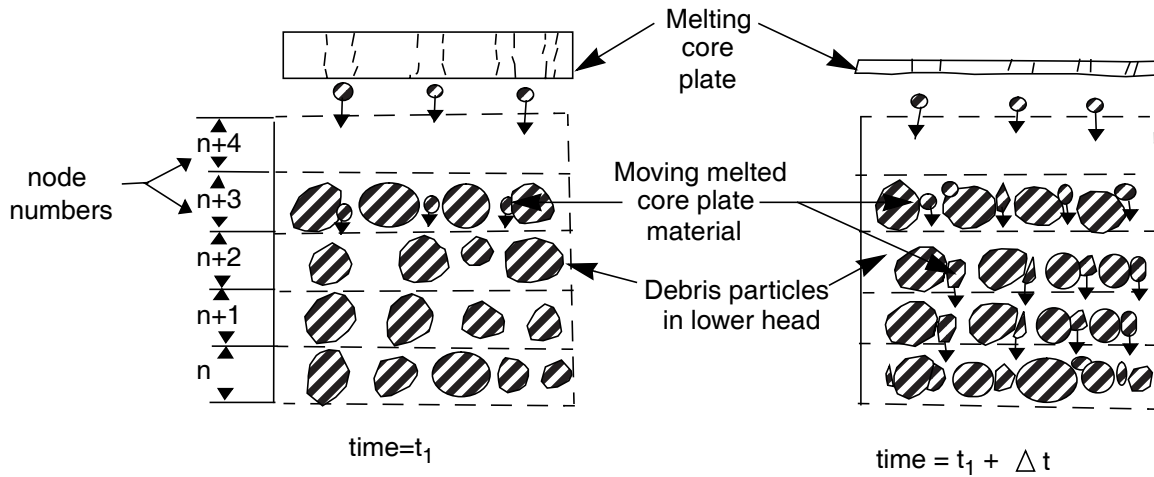


**Figure 1-3.** Extension in modeling of liquefied material within porous debris bed.

calculate the rate of melting of the core plate above the porous debris bed. The numerical solution for the processes being modeled are described in Section 5 and the basic features of its implementation are described in Section 6. Section 7 presents the testing and assessing of the implemented models. A summary of the extensions in modeling is presented in Section 8. The references are presented in Section 9.

## 2. Models for Movement of Material in Porous Debris

This section describes the models to be applied for calculating the movement liquefied core plate material through the interstices in a matrix of porous material. The system to be modeled has been previously shown in Figure 1-3. The movement of the liquefied material is driven by several forces, including gravity, capillary force, and pressure gradient. Resistances to movement are caused by viscous forces and form losses due to a continuous contraction and expansion of flow areas as the liquefied material flows through the porous debris. The resistances to movement increase with the velocity of the moving material. The balancing of the forces driving the movement of the liquefied material with the forces resisting the movement results in a conservation of momentum equation for the liquefied material.

The following assumptions are applied to simplify the modeling in a manner that maintains an accuracy of solution of the same order of magnitude as the uncertainties of governing material properties and debris behavior.

1. The porous medium is composed only of (U, Zr)O<sub>2</sub> particles.
2. The material permeating the porous medium is composed only of stainless steel.
3. Stainless steel does not chemically react with (U, Zr)O<sub>2</sub>.
4. The (U, Zr)O<sub>2</sub> particles do not melt.
5. The permeating stainless steel is in thermal equilibrium with the (U, Zr)O<sub>2</sub> particles it contacts.
6. Stainless steel does not permeate through any location with a temperature less than the freezing temperature of stainless steel (1700 K).
7. Stainless steel does not permeate through any location with a temperature greater than the melting temperature of (U, Zr)O<sub>2</sub> (~3000 K).
8. Gas does not flow through the porous debris bed.
9. Water is not present at any location with liquefied stainless steel.
10. Capillary forces are negligible.
11. The frictional drag on the liquefied stainless steel is balanced by the force of gravity, with the result of quasi-steady flow of the liquefied material through the voids in the debris bed; pressure drop due to acceleration of liquefied material is small compared to pressure drop due to gravity, and pressure drop due to momentum flux is small compared to pressure drop due to gravity.
12. The relative passability of the debris bed is equal to its relative permeability.
13. Liquefied stainless steel does not move in the radial direction; this assumption is based on the expectation of a small radial temperature gradient and debris characteristics uni-

form in the radial direction.

14. The effect of a wall (lower head) on the movement of the liquefied stainless steel is negligible.

In general, the assumptions are consistent with the expected behavior of the core plate and the expected characteristics of lower plenum debris. The omission of the inertial and capillary terms in the momentum equation is based on order of magnitude analyses; the results of these analyses are presented at the end of the section on numerical solution (Section 5), where results are calculated for representative cases.

Taking into account the above assumptions, the conservation of momentum equation for the liquefied material is given by the equation<sup>2,3</sup>

$$\frac{\mu_1 j}{k_1 k} + \frac{\rho_1 j^2}{m_1 m} = \rho_1 g \quad (2-1)$$

where

$\mu_1$	=	dynamic viscosity of liquefied material (kg/m · s),
$j$	=	superficial velocity of liquefied material (m/s),
$k$	=	Darcy permeability (m <sup>2</sup> ),
$k_1$	=	relative permeability (unitless),
$m$	=	passability of debris bed (m),
$m_1$	=	relative passability of debris bed (unitless),
$\rho_1$	=	density of liquefied material (kg/m <sup>3</sup> ),
$g$	=	acceleration of gravity (9.8 m/s <sup>2</sup> ).

The second term of the above equation is the turbulent drag counterpart to the viscous drag represented by the first term.

The Darcy permeability is calculated by the equation

$$k = \frac{\epsilon^3 D_p^2}{150(1 - \epsilon)^2} \quad (2-2)$$

where

$\varepsilon$  = porosity of the debris bed (unitless),

$D_p$  = diameter of particles in debris bed (m).

The passability of the debris bed is calculated by the equation

$$m = \frac{\varepsilon^3 D_p}{1.75(1 - \varepsilon)} \quad (2-3)$$

In general the relative passability is less than the relative permeability, but they are assumed to be equal for this analysis.<sup>4</sup> Thus,

$$m_l = k_l \quad (2-4)$$

The relative permeability is a function of the effective saturation of the debris bed and the Darcy permeability. The relative permeability is calculated by the equation<sup>2</sup>

$$\begin{aligned} k_l &= S_e^3, S_e > 0 \\ k_l &= 0, S_e \leq 0 \end{aligned} \quad (2-5)$$

where

$S_e$  = effective saturation of debris bed (unitless).

The effective saturation is calculated by the equation<sup>2</sup>

$$S_e = \frac{S - S_r}{1 - S_r} \quad (2-6)$$

where

$S_e$  = effective saturation of debris bed (unitless),

$S$  = true saturation of debris bed; volume fraction of liquefied material in pores of debris bed (unitless),

$S_r$  = residual saturation of debris bed (unitless).

The residual saturation,  $S_r$ , is a function of the surface tension of the liquid and of the degree of wetting of the solid material by the liquefied material. Reference 2 provides an empirical equation for calculating residual saturation that is appropriate for debris resulting from the disintegration of nuclear reactor cores. This equation is

$$S_r = \begin{cases} \frac{1}{86.3} \left[ \frac{\gamma \cos(\theta)}{k \rho_l g} \right]^{0.263} & ; 0 \leq \theta \leq 90^\circ \\ 0 & ; 90^\circ < \theta \leq 180^\circ \end{cases} \quad (2-7)$$

where

$\gamma$  = surface tension of the liquid (N/m),

$\theta$  = wetting contact angle (degrees).

In the case of liquefied material that does not wet the solid material ( $90^\circ < \theta < 180^\circ$ ), the residual saturation is equal to zero. An example of such a system is a debris bed composed of (U, Zr)O<sub>2</sub> and stainless steel.<sup>2</sup> In this case, bulk motion occurs at a relatively low values of bed saturation.

The conservation of mass equation is applied to obtain the relation of the rate of change with time of the local saturation of the debris bed to the local velocity of the liquefied debris and to the local rate of melting of the solid debris. The result is the equation

$$\frac{\partial S}{\partial t} = -\frac{1}{\varepsilon} \frac{\partial j}{\partial y} \quad (T_s < T_{sol}) \quad (2-8)$$

where

$t$  = time (s),

$y$  = spatial coordinate that defines elevation (defined in Figure 1-1)(m).

Equations (2-1) and (2-8) are a set of two equations for solving for the variables  $j$  and  $S$ . The terms  $k_l$  and  $m_l$  in Equation (2-1) are a function of  $S$  and thus contribute to the nonlinearity of the set of equations. Although the momentum equation in the model described in Reference 2 omits the turbulent term in Equation (2-1), a hand calculation for a possible debris bed condition indicated that for a saturated debris bed the omission of the turbulent term would result in a factor of three overprediction of the velocity of the liquefied material. These calculations are presented at the end of the section on the numerical solution (Section 5). So the turbulent term is being retained for the present model.

### 3. Effects of Material Movement on Debris Bed Heat Transfer

The movement of liquefied core plate material through the interstices in a porous debris bed results in the transport of energy within the debris bed. In addition, the movement of the liquefied material through the debris bed influences the thermal conductivity and heat capacity of the debris bed. As a result, the movement of liquefied material may have a significant influence on the temperature distribution within the debris bed. This section defines the change to be made to the heat transport equations in the COUPLE model<sup>1</sup> so as to account for the effect of material movement on temperature distribution.

The COUPLE model calculates the transport of heat through a porous medium by the equation

$$(\rho c_v)_e \frac{\partial T}{\partial t} = \frac{\partial}{\partial x} \left( K_e \frac{\partial T}{\partial x} \right) + \frac{\partial}{\partial y} \left( K_e \frac{\partial T}{\partial y} \right) + Q \quad (3-1)$$

where

$(\rho c_v)_e$	=	$(1 - \epsilon_h)(\rho c_v)_m$
$\rho$	=	density (kg/m <sup>3</sup> ),
$c_v$	=	constant volume specific heat (J/kg · K),
$K_e$	=	effective thermal conductivity (W/m · K),
$Q$	=	volumetric heat generation rate (W/m <sup>3</sup> ),
$T$	=	temperature of debris (K),
$\epsilon_h$	=	heat conduction porosity of debris ; $\epsilon(1 - S)$ (unitless),
$S$	=	saturation of debris bed,
$x$	=	spatial coordinate in horizontal direction (m),
$y$	=	spatial coordinate in vertical direction (m),
$m$	=	mixture of stainless steel and (U, Zr)O <sub>2</sub> .

The boundary conditions for equation (3-1) are defined by the code user. Boundary conditions are defined for the bottom and top surfaces, and left and right surfaces of the region being represented by the COUPLE model. The boundary conditions at these surfaces can be either adiabatic surface or convection and radiative heat transfer to fluid.<sup>1</sup> For the outer surface of a reactor vessel lower head submerged in water, the convective heat transfer is calculated using the Cheung model.<sup>5</sup> For other surfaces, the convective heat transfer is calculated by the RELAP5 convective heat transfer models.<sup>6</sup>

The above equation models heat transport through debris by conduction and radiation. To account for the transport of heat by the movement of liquefied material, the  $Q$  term in the above equation will be replaced by the term

$$Q_N = Q + Q_T \quad (3-2)$$

where

$$\begin{aligned} Q_N &= \text{net volumetric heat generation rate (W/m}^3\text{),} \\ Q_T &= \text{effective heat generation due to movement of liquefied material (W/m}^3\text{).} \end{aligned}$$

The variable  $Q_T$  in the above equation is a function of the rate of flow and internal energy of the liquefied material. The rate of flow of liquefied material into node  $n$  is calculated by the equation

$$M_F = 0.5(j_{n+1} + j_n)A\rho_1\Delta t \quad (3-3)$$

where

$$\begin{aligned} M_F &= \text{mass of liquefied material that flowed into node } n \text{ during time step (kg),} \\ j_{n+1} &= \text{superficial velocity of liquefied material at node } n+1 \text{ (m/s),} \\ A &= \text{average of cross sectional areas of nodes } n \text{ and } n+1 \text{ (m}^2\text{),} \\ \rho_1 &= \text{density of liquefied material flowing into node } n \text{ (kg/m}^3\text{),} \\ \Delta t &= \text{time step (s).} \end{aligned}$$

The above equation is formulated assuming that there is liquid material of only one type of composition, namely stainless steel.

The variable  $Q_T$  in Equation (3-2) at any node is then calculated by the equation

$$Q_{Tn} = M_F([u_l(T_F) - u_l(T_n)]/\Delta z_n\Delta t) \quad (3-4)$$

where

$$\begin{aligned} Q_{Tn} &= \text{effective heat generation due to movement of liquefied material at node } n \text{ (W/m}^3\text{),} \\ u_l(T_F) &= \text{internal energy of flowing liquefied material at its temperature of } T_F \text{ (J/kg)} \end{aligned}$$

(calculated by MATPRO function ZUNTH1),

$T_n$  = temperature of node n (K),

$A$  = cross sectional area ( $m^2$ ),

$\Delta z_n$  = height of node n (m).

The movement of liquefied material through the interstices of a porous debris bed influences the effective thermal conductivity of the debris bed.

The effective thermal conductivity is calculated by the equation

$$k_e = k_{ec} + k_r \quad (3-1)$$

where

$k_e$  = effective conductivity ( $W/m \cdot K$ ),

$k_{ec}$  = effective conductivity (conduction only) ( $W/m \cdot K$ ),

$k_r$  = radiative conductivity ( $W/m \cdot K$ ).

The Imura-Takegoshi<sup>7</sup> model for thermal conductivity is combined with the Vortmeyer<sup>8</sup> radiation model.

The Imura-Takegoshi model in equation form is given as follows:

$$k_{ec} = \left[ \Psi + \frac{1 - \Psi}{\phi + \frac{1 - \phi}{v}} \right] k_g \quad (3-2)$$

$$\phi = 0.3 \epsilon_h^{1.6} v^{-0.044} \quad (3-3)$$

$$v = \frac{k_s}{k_g} \quad (3-4)$$

$$\Psi = \frac{\epsilon_h - \phi}{1 - \phi} \quad (3-5)$$

where

- $k_g$  = thermal conductivity of vapor in pores ( $W/m \cdot K$ ),
- $k_s$  = thermal conductivity of mixture of stainless steel and  $(U, Zr)O_2$  ( $W/m \cdot K$ ),
- $\epsilon_h$  = porosity of debris for heat transfer calculations =  $\epsilon (1-S)$ .

The mixture thermal conductivity ( $k_s$ ) is calculated by the MATPRO function named ZUTCO1.<sup>9</sup>

The Vortmeyer model is given as

$$k_r = 4\eta\sigma D_p T^3 \quad (3-6)$$

where

- $\eta$  = radiation exchange factor (user-defined value, with default value of 0.8),
- $\sigma$  = Stefan-Boltzmann constant  $W/m^2 \cdot K^4$  ( $5.668 \times 10^{-8}$ ),
- $D_p$  = particle diameter (m),
- $T$  = temperature (K).

#### 4. Boundary Conditions for Case of Core Plate Melting Above Debris Bed

This section describes the boundary condition applied to the model for movement of liquefied core plate material through a ceramic porous debris bed below the core plate. Such a case is shown in Figure 4-1. For nodes at the top of the debris bed, the equation based on the principles of flow of liquefied material in a porous debris bed is replaced by an equation that defines the rate of melting of the core plate above the debris bed. In other words, Equation (3-3) in Section 3 is replaced by the equation

$$M_{FT} = AG\Delta t \quad (4-1)$$

where

- $M_{FT}$  = mass of liquefied material that flowed into a node at top of debris bed during time step (kg),
- $A$  = cross sectional area of the node ( $m^2$ ),
- $G$  = rate of melting of structure above debris bed per unit of cross sectional area ( $kg/s/m^2$ ),

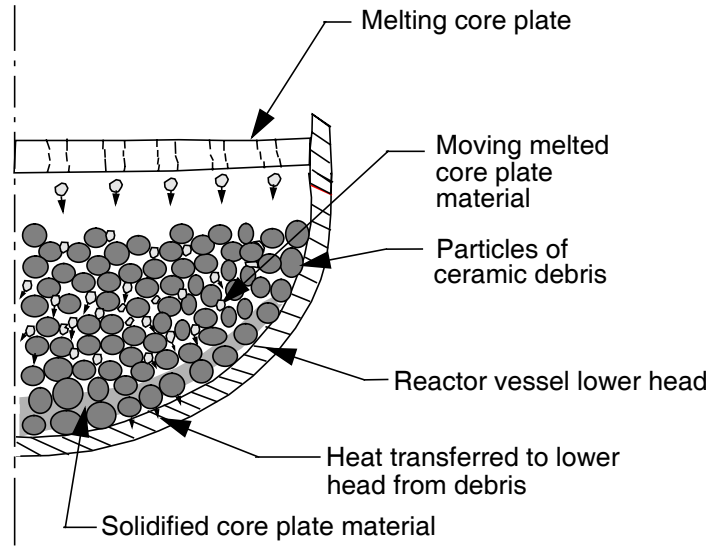


**Figure 4-1.** Schematic of material movement occurring when core plate melts and lower head supports ceramic porous debris.

$\Delta t$  = time step (s).

## 5. Numerical Solution

An explicit, iterative scheme for numerical solution is used to solve for the distribution in velocity and debris bed saturation. The scheme is based on the concept that the velocity gradient changes at a slower rate than the degree of bed saturation. In the first step for the first iteration, the change in bed saturation at each node is calculated using previous time step velocities in the neighborhood of each node. Next, the end of time step velocity at each node is calculated using the values for bed saturation calculated in the previous step. Next, the bed saturation at each node is calculated using the velocities just calculated for the end of the time step. If at any node the difference between the last two values calculated for bed saturation is greater than the tolerance for error in bed saturation, another iteration is performed. Subsequent iterations are performed until convergence is obtained at each node.

The equations in the numerical solution scheme are arranged as follows. First, a guess of the end of time step bed saturation is calculated using the equation

$$S_n^{m+1} = S_n^m - \frac{1}{\varepsilon} \left[ \frac{(j_{n+1}^m - j_{n-1}^m)}{(y_{n+1} - y_{n-1})} \right] \Delta t \quad (5-1)$$

where

$m$  = time step number,

$S_n^{m+1}$	=	bed saturation at node n at end of time step,
$S_n^m$	=	same as $S_n^{m+1}$ , but for start of time step,
$j_{n+1}^m$	=	superficial velocity at start of time step of liquefied material at node n+1 (m/s),
$j_n^m$	=	same as $j_{n+1}^m$ , but for node n (m/s),
$\varepsilon$	=	porosity for mass transport calculations (unitless),
$y_{n+1}$	=	elevation of node n+1 (m),
$y_n$	=	elevation of node n (m),
$\Delta t$	=	time step (s).

In the above equation, the nodes are assumed to have uniform cross sectional areas and uniform spacings in the vertical direction.

The moving of liquefied material changes the local porosity. Two categories of porosity need to be calculated at each node at each time step. One category of porosity, named the mass transport porosity, is used in the equations that calculate the flow of liquefied material. For this category, the volumes of liquid and gas are lumped together to represent the porosity. The other category of porosity, named the heat conduction porosity, is used in the equations that calculate the conduction of heat through the debris bed. For this category, the volumes of solid material and liquefied debris are lumped together.

The heat conduction porosity is related to the mass transport porosity by the equation

$$\varepsilon_h = \varepsilon(1 - S_n^{m+1}). \quad (5-2)$$

where

$\varepsilon_h$	=	heat conduction porosity (unitless),
$\varepsilon$	=	mass transport porosity (unitless),
$S_n^{m+1}$	=	saturation of debris bed (unitless).

Next, the Darcy permeability and the passability of the debris bed are updated using the equations

$$k_n = \frac{\varepsilon^3 D_p^2}{150(1 - \varepsilon)^2} \quad (5-3)$$

$$m_n = \frac{\varepsilon^3 D_p}{1.75(1 - \varepsilon)} \quad (5-4)$$

where

$k_n$  = Darcy permeability of debris bed at node n ( $m^2$ ),

$m_n$  = passability of debris bed at node n (m).

Next, the effective saturation of the debris bed at the end of the time step for each node is calculated using the equation

$$S_{en}^{m+1} = \frac{S_n^{m+1} - S_r}{1 - S_r} \quad (5-5)$$

where

$S_{en}^{m+1}$  = effective saturation at node n at end of time step.

The residual saturation,  $S_r$ , is a function of material properties, namely wetting angle, surface tension, Darcy permeability, and liquid density; it is calculated using Equation (2-7).

Next, the relative permeability of the debris bed at the end of the time step for each node is calculated using the equation

$$k_{ln}^{m+1} = [S_{en}^{m+1}]^3 \quad (5-6)$$

where

$k_{ln}^{m+1}$  = relative permeability at node n at end of time step,

The relative passability of the debris bed at the end of the time step for each node is calculated using the equation

$$m_{ln}^{m+1} = k_{ln}^{m+1} \quad (5-7)$$

where

$m_{ln}^{m+1}$  = relative passability of debris bed at node n at end of time step.

Next, the velocity of the liquefied material at each node is calculated using Equation (2-1). For numerical solution, terms in this equation are combined as follows

$$A[j_n^{m+1}]^2 + B j_n^{m+1} + C = 0 \quad (5-8)$$

where

$$\begin{aligned} A &= \frac{\rho_l}{m_{ln}^{m+1} m_n} \\ B &= \frac{\mu_l}{k_{ln}^{m+1} k_n} \\ C &= -\rho_l g \\ \rho_l &= \text{density of liquefied debris (kg/m}^3\text{)}, \\ \mu_l &= \text{dynamic viscosity of liquefied material kg/m} \cdot \text{s)}, \\ g &= \text{acceleration of gravity (9.8 m/s}^2\text{)}. \end{aligned}$$

Applying the quadratic equation, the superficial velocity of the liquefied material at each node at the end of the time step is calculated using the equation

$$j_n^{m+1} = \frac{-B \pm [B^2 - 4AC]^{0.5}}{2A} \quad (5-9)$$

The above equation has two values; since the liquefied material can only flow down, only the positive value is applied.

The bed saturation at each node at the end of the time step is then calculated using Equation (5-1) with the start of time step superficial velocities in this equation replaced with the end of time superficial velocities calculated by Equation (5-9).

The fractional difference in bed saturation between two successive iterations is calculated by the equation

$$f_n = \frac{|S_n^{i+1} - S_n^i|}{0.5(S_n^{i+1} + S_n^i)} \quad (5-10)$$

where

$$f_n = \text{fractional difference in value of } S_n^{m+1} \text{ between two successive iterations,}$$

$i$  = iteration number,

$S_n^i$  = value of  $S_n^{m+1}$  at  $i$ -th iteration.

If the value of  $f_n$  at any node is greater than the tolerance in error for bed saturation, another iteration is performed.

After convergence of the debris bed saturation at each node has been obtained, the effect of the movement of liquefied material during the time step on heat transport is calculated. First, the mass of material flowing into each node during the time step is calculated. For the top node in the debris bed, Equation (4-1) is used to calculate the mass of liquefied material that moved into this node during the time step. Then, Equation (3-4) is used to calculate the term added to the volumetric heat generation rate for each axial node to account for the transport of liquefied material. Then, the heat conduction porosity for each node is updated to account for the addition or subtraction of material from each node during the time step. Then, the atomic fractions of stainless steel and (U, Zr)O<sub>2</sub> at each node are updated to account for the addition or subtraction of material from each node during the time step. The particle size at each node is assumed to not be influenced by the presence of liquefied debris or frozen previously liquefied debris.

The mass of liquefied material added to or subtracted from each node is calculated by the equation

$$m_{an} = A\rho_l \left( j_{n+1}^{m+1} - j_{n-1}^{m+1} \right) \Delta t \quad (5-11)$$

where

$m_{an}$  = mass of liquefied material added to node  $n$  during time step (kg),

$A$  = cross sectional area of nodes (m<sup>2</sup>).

For the top node in the debris bed, the mass of liquefied material flowing into this node is calculated by the equation

$$m_{an} = AG\Delta t \quad (5-12)$$

where

$G$  = rate of melting of structure above the debris bed per unit of cross sectional area (kg/s)/m<sup>2</sup>.

To assure conservation of mass, the numerical solution is begun from the bottom most node and proceeds upward. At the bottom most node, the boundary condition of an impermeable boundary is imposed. Thus, the change in mass of stainless steel at this location is calculated by the equation

$$m_{a1} = 0.5A\rho_l(j_2^{m+1})\Delta t \quad (5-13)$$

The change in mass of stainless steel at other nodes is calculated using the mass added to the node below. Thus, the change in mass at axial node 2 is calculated by the equation

$$m_{a2} = (0.5A\rho_l(j_3^{m+1} + j_2^{m+1})\Delta t - m_{a1}) \quad (5-14)$$

Three constraints are applied to the motion of liquefied material. First, if the temperature at a location is less than the melting temperature of stainless steel, then that location is impermeable. Second, if liquid water is present at a location, then that location is impermeable. Third, if the temperature at any location is greater than the melting temperature of a mixture of  $UO_2$  and  $ZrO_2$ , then that location is impermeable. In general, if the condition for the second constraint is satisfied, then the condition for the first constraint is also satisfied. The third constraint is based on the assumption that melted (U, Zr) $O_2$  will flow a small distance, freeze, and form an impermeable crust. These constraints are applied by the equation

$$j_n^{m+1} = 0 \begin{cases} T_n < T_{ms} \\ T_n > T_{mu} \\ \alpha_f > 0 \end{cases}$$

where

$$\begin{aligned} T_{ms} &= \text{melting temperature of stainless steel (1671 K),} \\ T_{mu} &= \text{melting temperature of mixture of } UO_2 \text{ and } ZrO_2 \text{ (~3000 K),} \\ \alpha_f &= \text{volume fraction of liquid water.} \end{aligned}$$

If a crust of frozen (U, Zr) $O_2$  existed at a location before the melting of the core plate began, then that location is implicitly represented as impermeable from the assignment of a porosity of zero for that location.

Next, the calculation is made of the term to be added to the volumetric heat generation at each node to account for the thermal effect of the addition by flow of liquefied material to each node. This term is calculated by the equation

$$Q_{Tn} = m_{an}[u_l(T_F) - u_l(T_n)]/0.5(y_{n+1} - y_{n-1})A\Delta t \quad (5-15)$$

where

$$Q_{Tn} = \text{heat transported into node } n \text{ due to movement of liquefied material (W/m}^3\text{),}$$

$$\begin{aligned}
u_l(T_F) &= \text{internal energy of material flowing into node } n \text{ at temperature of } T_F \text{ (J/kg),} \\
T_F &= T_{n+1} \text{ (Temperature at node } n+1 \text{) for nodes other than top node; for top node,} \\
&\quad T_F = \text{temperature of material slumping onto top of debris bed (K),} \\
T_n &= \text{temperature of node } n \text{ (K).}
\end{aligned}$$

Next, the calculation is made of the atomic fractions of stainless steel and (U, Zr)O<sub>2</sub> at each node. The mass of stainless steel at each node at the end of a time step is calculated by the equation

$$m_{sn} = m_{sno} + m_{an} \quad (5-16)$$

where

$$\begin{aligned}
m_{sn} &= \text{mass of stainless steel at node } n \text{ at end of time step (kg),} \\
m_{sno} &= \text{mass of stainless steel at node } n \text{ at start of time step (kg).}
\end{aligned}$$

The atomic fractions are calculated by the equation

$$f_{sn} = \frac{m_{sn}}{a_{ws}} \left[ \frac{m_{sn}}{a_{ws}} + \frac{m_{un}}{a_{wu}} + \frac{m_{zn}}{a_{wz}} \right] \quad (5-17)$$

$$f_{zn} = \frac{m_{zn}}{a_{wz}} \left[ \frac{m_{sn}}{a_{ws}} + \frac{m_{un}}{a_{wu}} + \frac{m_{zn}}{a_{wz}} \right] \quad (5-18)$$

$$f_{un} = 1 - f_{sn} - f_{zn} \quad (5-19)$$

where

$$\begin{aligned}
f_{sn} &= \text{atomic fraction of stainless steel at node } n \text{ at end of time step,} \\
a_{ws} &= \text{atomic weight of stainless steel (56),} \\
m_{un} &= \text{mass of UO}_2 \text{ at axial node } n \text{ (kg),} \\
a_{wu} &= \text{atomic weight of UO}_2 \text{ (270),} \\
f_{un} &= \text{atomic fraction of UO}_2, \\
f_{zn} &= \text{atomic fraction of ZrO}_2
\end{aligned}$$

$m_{zn}$  = mass of  $ZrO_2$  at node n (kg),

$a_{wz}$  = atomic weight of  $ZrO_2$  (123.2).

In order to estimate the rate of movement of melted stainless steel through a medium of porous debris, Equation (5-8) was solved for two representative cases. In both cases, the debris and melted stainless steel are assumed to have the characteristics and properties<sup>4</sup> shown in Table 5-1. The solution was made for two values of effective saturation, namely  $S_e = 0.1$  and  $S_e = 1.0$ . The substitution of these values into the equations for the coefficients in Equation (5-8) gives the results shown in Table 5-2. The superficial velocities for the two values of effective saturation are shown in Table 5-3. The superficial velocities ranged from  $9.7 \times 10^{-5}$  m/s to  $2.9 \times 10^{-2}$  m/s. The table also shows the values calculated for superficial velocity when turbulent drag is neglected. For an effective saturation of 1.0, turbulent drag reduces the superficial velocity by a factor of three.

**Table 5-1.** Characteristics and properties for debris and melted stainless steel for scoping calculations.

Characteristic or property	Symbol	Units	Value
<i>porosity of debris</i>	$\epsilon$	-	0.4
<i>diameter of debris particles</i>	$D_p$	m	$2 \times 10^{-3}$
<i>density of liquefied stainless steel</i>	$\rho_l$	kg/m <sup>3</sup>	6920
<i>viscosity of liquefied stainless steel</i>	$\mu_l$	kg/m · s	$3.2 \times 10^{-3}$
<i>wetting angle of liquefied stainless steel in contact with (U, Zr)O<sub>2</sub></i>	$\theta$	degrees	120
<i>surface tension of liquefied stainless steel</i>	$\gamma$	N/m	0.45
<i>heat capacity of liquefied stainless steel</i>	$c_{pl}$	(J)/kg · K	690
<i>thermal conductivity at liquefied stainless steel</i>	$\lambda$	W/m · K	20

**Table 5-2.** Values of coefficients in Equation (5-8) for two representative cases.

Effective saturation	A	B	C
0.1	$5.67 \times 10^{10}$	$6.77 \times 10^8$	$-6.78 \times 10^4$
1.0	$5.67 \times 10^7$	$6.77 \times 10^5$	$-6.78 \times 10^4$

**Table 5-3.** Superficial velocities for two representative cases.

Effective saturation	Superficial velocity(m/s)	
	Turbulent drag	No turbulent drag
<i>0.1</i>	$9.7 \times 10^{-5}$	$1.0 \times 10^{-4}$
<i>1.0</i>	$2.9 \times 10^{-2}$	<i>0.10</i>

The relatively slow movement of the liquefied stainless steel allows the inertial terms to be neglected in the momentum equation without significant loss of accuracy. For the case of saturated debris, which results in an upper bound on the velocity of the liquefied stainless steel, the gravity and viscous terms in the momentum equation are of order of  $5 \times 10^4 \text{ N/m}^3$ , while the inertial terms<sup>3</sup> are estimated to be of order of  $1 \times 10^3 \text{ N/m}^3$ .

Inclusion in the the calculations of capillary forces would not significantly change the velocities shown in Table 5-3. The capillary forces are a function of the porosity and particle size of the debris, surface tension of the liquid stainless steel, and the wetting angle of liquefied stainless steel in contact with (U, Zr)O<sub>2</sub>.<sup>2,3</sup> The values of the latter two properties are not firmly established.<sup>2</sup> Assuming values for these latter two properties that result in an upper bound on the capillary forces, and assuming a gradient in effective saturation of 10.0/m, the capillary force term in the momentum equation is estimated to be of order of  $0.7 \times 10^4 \text{ N/m}^2$ , which is an order of magnitude smaller than the gravitational and viscous terms.

The relatively slow movement of the liquefied stainless steel justifies the assumption of thermal equilibrium between the stainless steel and the (U, Zr)O<sub>2</sub>. The time constant for conduction heat transfer to the stainless steel in the interstices of the porous debris is approximated by the equation

$$\tau = \frac{\rho_1 c_{pl} (\Delta x)^2}{6\lambda} \quad (5-20)$$

where

$\tau$  = time constant (s),

$\rho_1$  = density of liquefied stainless steel ( $6920 \text{ kg/m}^3$ ),

$c_{pl}$  = heat capacity of liquefied stainless steel ( $690 \text{ J/kg} \cdot \text{K}$ ),

$\Delta x$  = average thickness of interstices, which is estimated to be approximately equal to the diameter of the UO<sub>2</sub> particles ( $2 \times 10^{-3} \text{ m}$ ),

$\lambda$  = thermal conductivity of liquefied stainless steel ( $20 \text{ W/m} \cdot \text{k}$ ).

The time constant for conduction heat transfer is calculated to be 0.16 s. Assuming a maximum temperature gradient in the (U, Zr)O<sub>2</sub> of 1000 K/m, the liquefied stainless steel needs to flow for 34 s

before experiencing a factor to two change in its ambient temperature. This order of magnitude larger time than the time constant for conduction heat transfer indicates that the assumption of thermal equilibrium of the stainless steel and (U, Zr)O<sub>2</sub> is justified.

## 6. Implementation into COUPLE model

This section identifies the extensions made to the data base of the COUPLE model and to its subroutines in order to implement the numerical solution for the movement of liquefied core plate material through a porous debris bed. The variables added to the COUPLE model data base are described in Table 6-1. This table also defines the Fortran name assigned each variable added to the COUPLE data base and identifies its corresponding name in the numerical solution section of this report. The table also identifies the subroutines that calculate the values of the new variables. The arrays in Table 6-1 are stored in the COUPLE bulk storage array named “a,” which is stored in the common block named “alcm.” The pointers in Table 6-1 are stored in the COUPLE common block named “iparm.” In order to improve computational efficiency, several variables in the numerical solution are omitted from Table 6-1, such as (1) density of liquid material, and (2) dynamic viscosity of liquid material. These variables are stored as local variables in the subroutines that use them.

**Table 6-1.** Variables added to COUPLE data base for modeling of flow of liquefied material within porous debris bed .

variable definition	Fortran name	Numerical solution name	units	subroutines that calculate variable
<i>pointer to variable storing bed saturation at current iteration at element n</i>	<i>iptbst</i>	-	-	<i>AUMESH</i>
<i>bed saturation at element n at current iteration</i>	<i>a(iptbst+n-1)</i>	$S_n^m + I$	-	<i>MOVCP</i>
<i>pointer to variable storing bed saturation at previous iteration</i>	<i>iptbs0</i>	-	-	<i>AUMESH</i>
<i>bed saturation at element n at previous iteration</i>	<i>a(iptbs0+n-1)</i>	$S_n^m$	-	<i>MOVCP</i>
<i>pointer to variable storing effective bed saturation at element n</i>	<i>iptebs</i>	-	-	<i>AUMESH</i>
<i>effective bed saturation at element n</i>	<i>a(iptebs+n-1)</i>	$S_{en}$	-	<i>MOVCP</i>
<i>pointer to array storing Darcy permeability at element n</i>	<i>iptprm</i>	-	-	<i>AUMESH</i>
<i>Darcy permeability at element n</i>	<i>a(iptprm+n-1)</i>	$k_n$	$m^2$	<i>MOVCP</i>
<i>pointer to array storing passability at element n</i>	<i>iptpas</i>	-	-	<i>AUMESH</i>

**Table 6-1.** Variables added to COUPLE data base for modeling of flow of liquefied material within porous debris bed (continued).

variable definition	Fortran name	Numerical solution name	units	subroutines that calculate variable
<i>passability at element n</i>	<i>a(iptpas+n-1)</i>	$m_n$	<i>m</i>	<i>MOVCPL</i>
<i>pointer to variable storing relative permeability at element n</i>	<i>iptrpr</i>	-	-	<i>AUMESH</i>
<i>relative permeability at element n</i>	<i>a(iptrpr+n-1)</i>	$k_{ln}$	-	<i>MOVCPL</i>
<i>pointer to array storing mass of stainless steel in element n</i>	<i>iptmss</i>	-	-	<i>AUMESH</i>
<i>mass of stainless steel in element n</i>	<i>a(iptmss+n-1)</i>	-	<i>kg</i>	<i>MUPDAT, MOVCPL</i>
<i>pointer to array storing mass of (U, Zr)O<sub>2</sub> in element n</i>	<i>iptmuo</i>	-	-	<i>AUMESH</i>
<i>mass of (U, Zr)O<sub>2</sub> in element n</i>	<i>a(iptmuo+n-1)</i>	-	<i>kg</i>	<i>MUPDAT, MOVCPL</i>
<i>pointer to array storing superficial velocity of liquefied material after current iteration at node n</i>	<i>iptjlm</i>	-	-	<i>AUMESH</i>
<i>superficial velocity of liquefied material at end of current time step at node n</i>	<i>a(iptjlm+n-1)</i>	$j_n^{m+1}$	<i>m/s</i>	<i>MUPDAT, MOVCPL</i>
<i>pointer to array storing superficial velocity of liquefied material after previous iteration at node n</i>	<i>iptjl0</i>	-	-	<i>AUMESH</i>
<i>superficial velocity of liquefied material at start of current time step at node n</i>	<i>a(iptjl0+n-1)</i>	$j_n^m$	<i>m/s</i>	<i>MOVCPL</i>

Several user-defined variables are required for the numerical solution; these variables are identified in Table 6-2. Two of the variables in Table 6-2 are material properties that are not defined in the material properties part (MATPRO)<sup>9</sup> of SCDAP/RELAP5. These variables are the liquid-solid contact angle and the surface tension of liquefied stainless steel. When the values of these material properties are firmly established, the values will be obtained from MATPRO instead of being user-defined. Another variable in this table, namely the rate of melting of the core plate above a debris bed can be obtained from calculations performed by the core plate model in SCDAP/RELAP5. Nevertheless, it is useful to make this variable

user-defined for testing and for analyses focusing on behavior of debris in the lower head of a reactor vessel instead of on behavior of an overall reactor system.

**Table 6-2.** User-defined variables added to data base for modeling of flow of liquefied material within porous debris bed .

Variable definition	Fortran name	Numerical solution or theory name	Units	Common block
<i>liquid-solid contact angle (wetting angle)</i>	<i>thtwet</i>	$\theta$	<i>radians</i>	<i>tblsp</i>
<i>surface tension of liquefied material</i>	<i>gamwet</i>	$\gamma$	<i>N/m</i>	<i>tblsp</i>
<i>rate of slumping of melting structure located directly above debris bed</i>	<i>mdtstr</i>	<i>G</i>	<i>(kg/s)/m<sup>2</sup></i>	<i>tblsp</i>
<i>accuracy of calculated bed saturation</i>	<i>accbst</i>	-	-	<i>tblsp</i>

The model for calculating the movement of liquefied stainless steel was programmed in a new subroutine named MOVCP. This new subroutine is called from subroutine COUPLE just before the call to subroutine EGEN2. The new subroutine calculates the distribution of liquefied stainless steel within the debris bed and calculates the addition or subtraction to be made to the volumetric heat generation term in the COUPLE model in order to account for the transport of heat by movement of liquefied material. The new subroutine also calculates the change in effective thermal conductivity and heat capacity at each node due to movement of liquefied material. The Fortran programming of the new subroutine is based on the numerical solution scheme outlined in Section 5 of this report.

The extensions made to existing COUPLE subroutines are summarized in Table 6-3. Subroutine MATERL was extended to define input needed for the models that calculate the movement of liquefied material. Subroutine AUMESH was extended to reserve storage for the new variables added to the COUPLE model to calculate the movement of liquefied material and its consequences. Subroutine ICPL was extended to initialize the new variables added to the COUPLE model. Subroutine COUPLE was extended to call the new subroutine named MOVCP, which calculates the movement of liquefied material and its consequences. Subroutine MAJCOU was extended to display the results calculated by subroutine MOVCP.

**Table 6-3.** Extensions to existing COUPLE subroutines for modeling flow of liquefied material within porous debris bed .

Subroutine	Line in subroutine	Extensions
<i>MATERL</i>	<i>read(eoin,1005)emissm</i>	<i>add to this read statement the definition of input variables listed in Table (6-3)</i>

**Table 6-3.** Extensions to existing COUPLE subroutines for modeling flow of liquefied material within porous debris bed (continued).

Subroutine	Line in subroutine	Extensions
<i>AUMESH</i>	<i>i111=i110+4*numel</i>	<i>after this line, define pointers listed in Table (6-2) and reserve storage for variables associated with the pointers</i>
<i>ICPL</i>	<i>do 50 i=1,numel</i>	<i>in this do loop, initialize to value of zero the variables in Table (6-2) with element number for index</i>
<i>COUPLE</i>	<i>call egen2(a(i8),....</i>	<i>before this line, add call to new subroutine named MOVCPPL to obtain movement of liquefied material and its consequences</i>
<i>MAJCOU</i>	<i>1575 format(... end if</i>	<i>after these lines, print values of bed saturation and porosity in each element and velocity of liquefied stainless steel</i>

## 7. Testing and Assessment of Implemented Models

The models added to SCDAP/RELAP5 will be tested and assessed using two test problems. The matrix of test problems is described in Table 7-1.

**Table 7-1.** Matrix of test problems for assessing models of liquefied material moving through porous debris bed .

Problem no.	Problem description	Focus of assessment
<i>1</i>	<i>Liquefied stainless steel slumps onto top of hot porous debris bed composed of (U, Zr)O<sub>2</sub> and then flows through the debris bed</i>	<i>Internal consistency of modeling, including maintaining of conservation of mass and energy</i>
<i>2</i>	<i>Except for porosity and particle size, same as Problem No. 1</i>	<i>Evaluate sensitivity of results to debris characteristics, rate of melting of core plate and convergence criterion</i>

The first problem involves the calculation of the flow of liquefied stainless steel that slumps onto the top of a porous debris bed. The test problem is described in Figure 7-1. The debris bed has an initial

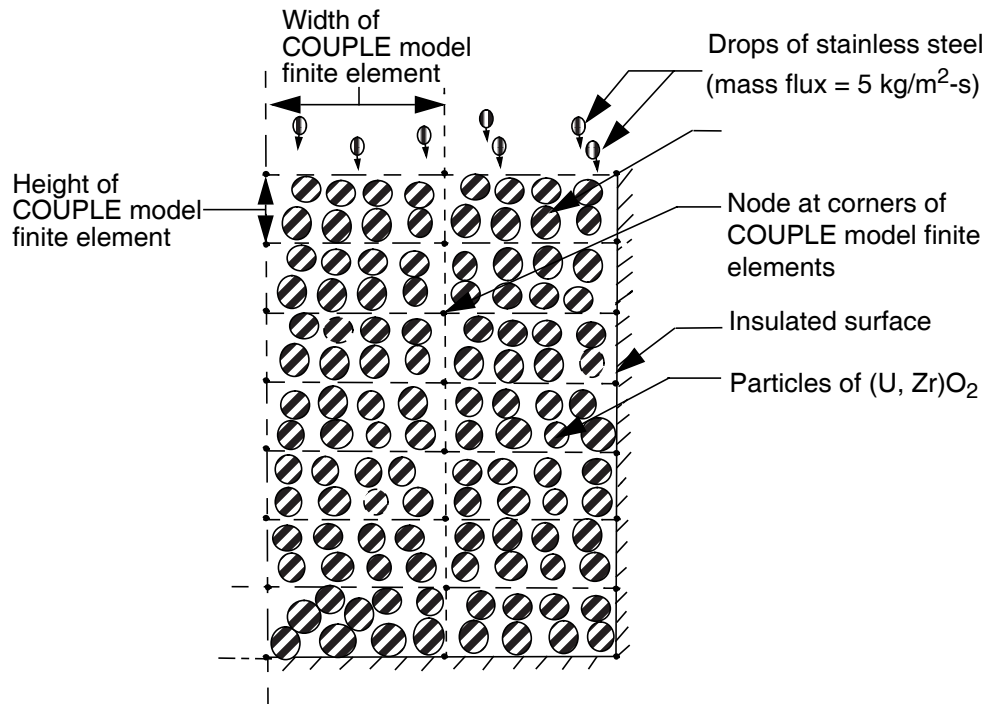


**Figure 7-1.** Description of Test Problem Number 1.

temperature of 2500 K and the slumping liquefied stainless steel has a temperature of 1700 K just before contact with the top surface of the debris bed. The debris particles have a volumetric heat generation rate of  $1 \text{ MW/m}^3$ . The debris particles are composed of  $(\text{U, Zr})\text{O}_2$  with a diameter of 2 mm. The initial porosity of the debris bed is 0.5. No water or steam is flowing through the debris bed. The debris is represented by two parallel stacks of COUPLE model finite elements, with twenty elements in each stack.

The second problem evaluates the sensitivity of calculated results to debris characteristics, rate of melting of the core plate, and convergence criterion.

## 8. Summary

Designs were described for models to calculate the movement of liquefied core plate through the interstices of porous debris composed of  $(\text{U, Zr})\text{O}_2$  particles. The models are intended for implementation into the COUPLE model in SCDAP/RELAP5 so as to give it the capability to calculate the effect on lower head heatup of liquefied core plate material moving through porous debris in the lower head. Equations and solution methods were presented for the calculation of the motion of liquefied and the heat transported by the moving material. The liquefied material is calculated to move until either it freezes, reaches a location in the debris bed where the degree of bed saturation is less than the residual saturation, or reaches an impermeable boundary. Equations were also presented for calculating the effect of moving material on effective thermal conductivity and heat capacity. A description was presented of the extensions in COUPLE model Fortran programming required to implement these equations and solution methods. A matrix of test problems was defined for assessing these models and their implementation.

## 9. References

1. The SCDAP/RELAP5 Development Team, "SCDAP/RELAP5/MOD3.2 Code Manual, Volume 2: Damage Progression Model Theory," NUREG/CR-6150, Volume 2, Rev. 1, INEL-96/0422, July 1998.
2. R. C. Schmidt and R. D. Gasser, "Models and Correlations of the DEBRIS Late-Phase Melt Progression Model," SAND93-3922, September 1997.
3. L. J. Siefken, "SCDAP/RELAP5 Modeling of Movement of Melted Material Through Porous Debris in Lower Head," INEEL/EXT-98-01178, December 1998.
4. Mo Chung and Ivan Catton, "Post-Dryout Heat Transfer in a Multi-Dimensional Porous Bed," Nuclear Engineering and Design 128 (1991) pages 289-304.
5. F. B. Cheung, K. H. Hadded, and Y. C. Liu, "A Scaling Law for the Local CHF on the External Bottom Side of a Fully Submerged Reactor Vessel," NUREG/CP-0157, Vol. 2, February 1997, pp. 253-277.
6. The RELAP5 Development Team, "RELAP5 Code Manual, Models and Correlations," NUREG/CR-5535, Vol. 4, August 1995.
7. S. Imura and E. Takegoski, "Effect of Gas Pressure on the Effective Thermal Conductivity of Packed Beds," Heat Transfer Japanese Research, 3, 4, 1974, p. 13.
8. D. Vortmeyer, "Radiation in Packed Solids," 6th International Heat Transfer Conference, Toronto, Canada, 1978.
9. The SCDAP/RELAP5 Development Team, "SCDAP/RELAP5/MOD3.2 Code Manual, Volume 4: MATPRO - A Library of Materials Properties for Light-Water-Reactor Accident Analysis," NUREG/CR-6150, Volume 4, Rev. 1, INEL-96/0422, July 1998



# 1. Introduction

In the event of a severe accident in a Light Water Reactor (LWR), particles of a ceramic mixture of  $\text{UO}_2$  and  $\text{ZrO}_2$  may stack in the lower head of the reactor vessel and form a porous debris bed. The context of the porous debris bed is shown in Figure 1-1. The slumping of jets of a mixture of molten  $(\text{U,Zr})\text{O}_2$  into a pool of water in the lower head is an example of a reactor core degradation event that may occur during a severe accident and result in the configuration of material shown in Figure 1-1. If the severe accident is not terminated, then eventually the core plate may melt and slump onto the top of the bed of ceramic particles. The core plate is generally composed of stainless steel and thus melts at a much lower temperature than the particles of  $(\text{U, Zr})\text{O}_2$  (1700 K versus ~3000 K). The subsequent heatup of the debris bed and lower head is a function of the extent to which the melted core plate permeates into the bed of  $(\text{U, Zr})\text{O}_2$  particles. This report describes a model for calculating the permeation of the melted core plate material into the porous debris bed and describes the implementation of this model into the existing model in the SCDAP/RELAP5 code<sup>1</sup> for calculating the heatup of the debris bed and lower head supporting the debris bed.

The COUPLE model in SCDAP/RELAP5 calculates the heatup of the lower head and the debris that it supports. The system that the COUPLE model is designed to analyze is shown in Figure 1-1. Previously

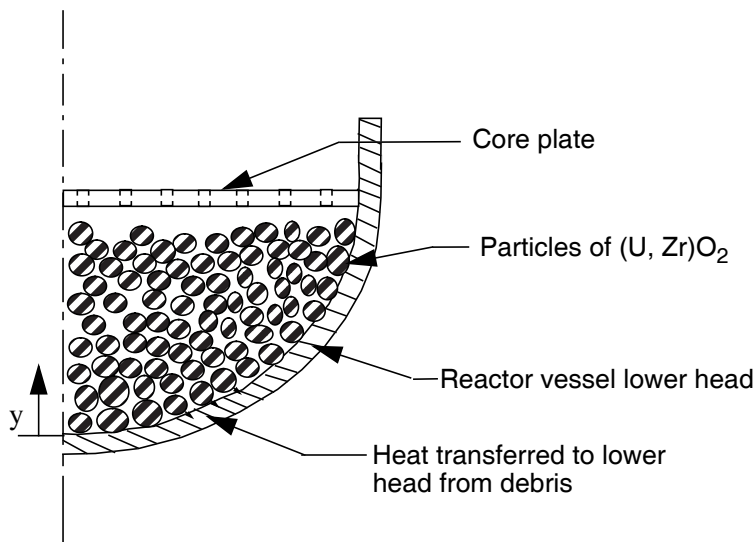


**Figure 1-1.** Schematic of system represented by COUPLE model (particle size of debris greatly exaggerated).

the COUPLE model could not calculate the movement of melted material. A schematic of the previous modeling capability with respect to melted material is shown in Figure 1-2. The schematic of modeling capability added to the COUPLE model is shown in Figure 1-3.

This report is organized as follows. Section 2 describes the models applied to calculate the movement of liquefied core plate material through the interstices in a matrix of porous  $(\text{U, Zr})\text{O}_2$  debris. Section 3 describes the effect of liquefied material movement on debris bed heat transfer. Section 4 describes the interface of the COUPLE model for the movement of liquefied material with models that

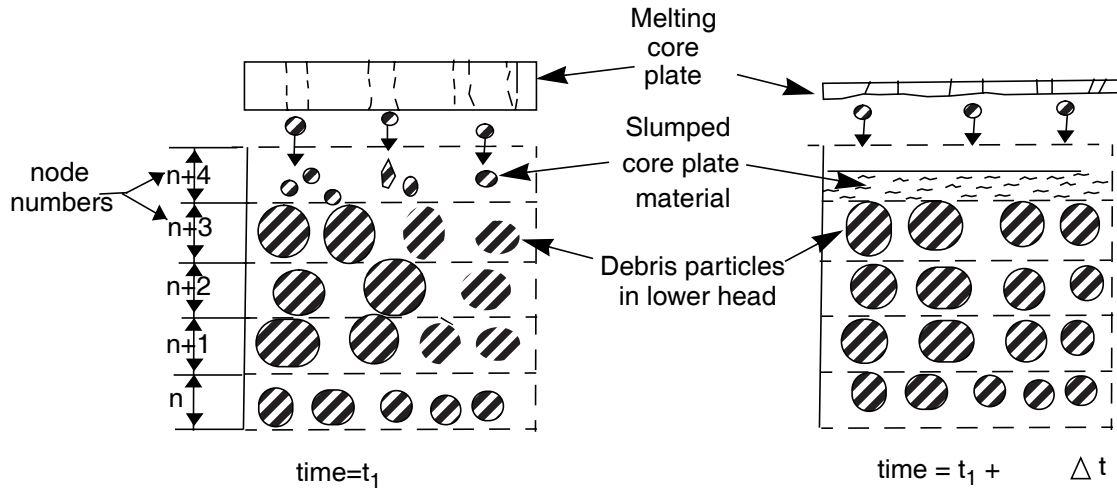


**Figure 1-2.** Previous modeling of liquefied material within porous debris bed.

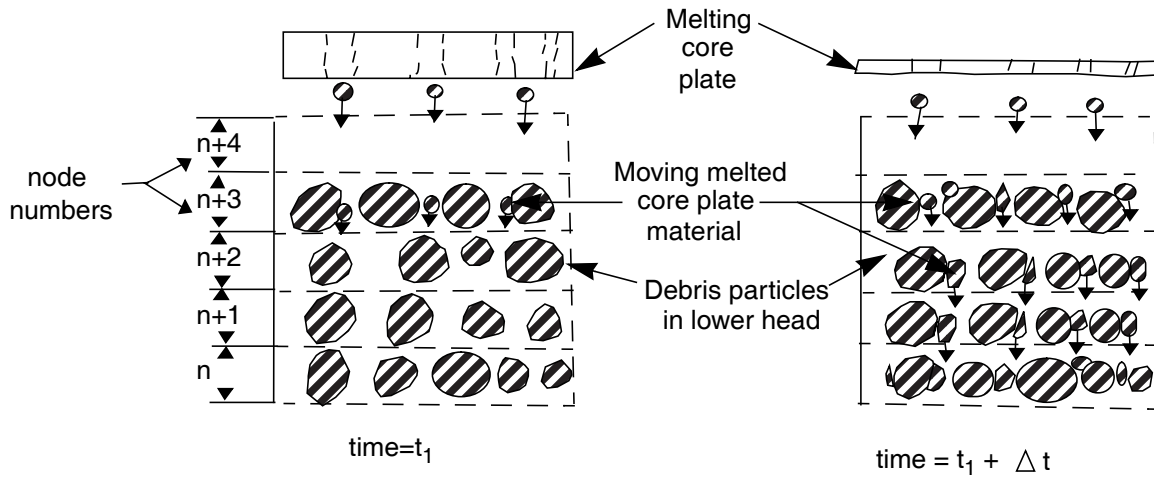


**Figure 1-3.** Extension in modeling of liquefied material within porous debris bed.

calculate the rate of melting of the core plate above the porous debris bed. The numerical solution for the processes being modeled are described in Section 5 and the basic features of its implementation are described in Section 6. Section 7 presents the testing and assessing of the implemented models. A summary of the extensions in modeling is presented in Section 8. The references are presented in Section 9.

## 2. Models for Movement of Material in Porous Debris

This section describes the models to be applied for calculating the movement liquefied core plate material through the interstices in a matrix of porous material. The system to be modeled has been previously shown in Figure 1-3. The movement of the liquefied material is driven by several forces, including gravity, capillary force, and pressure gradient. Resistances to movement are caused by viscous forces and form losses due to a continuous contraction and expansion of flow areas as the liquefied material flows through the porous debris. The resistances to movement increase with the velocity of the moving material. The balancing of the forces driving the movement of the liquefied material with the forces resisting the movement results in a conservation of momentum equation for the liquefied material.

The following assumptions are applied to simplify the modeling in a manner that maintains an accuracy of solution of the same order of magnitude as the uncertainties of governing material properties and debris behavior.

1. The porous medium is composed only of (U, Zr)O<sub>2</sub> particles.
2. The material permeating the porous medium is composed only of stainless steel.
3. Stainless steel does not chemically react with (U, Zr)O<sub>2</sub>.
4. The (U, Zr)O<sub>2</sub> particles do not melt.
5. The permeating stainless steel is in thermal equilibrium with the (U, Zr)O<sub>2</sub> particles it contacts.
6. Stainless steel does not permeate through any location with a temperature less than the freezing temperature of stainless steel (1700 K).
7. Stainless steel does not permeate through any location with a temperature greater than the melting temperature of (U, Zr)O<sub>2</sub> (~3000 K).
8. Gas does not flow through the porous debris bed.
9. Water is not present at any location with liquefied stainless steel.
10. Capillary forces are negligible.
11. The frictional drag on the liquefied stainless steel is balanced by the force of gravity, with the result of quasi-steady flow of the liquefied material through the voids in the debris bed; pressure drop due to acceleration of liquefied material is small compared to pressure drop due to gravity, and pressure drop due to momentum flux is small compared to pressure drop due to gravity.
12. The relative passability of the debris bed is equal to its relative permeability.
13. Liquefied stainless steel does not move in the radial direction; this assumption is based on the expectation of a small radial temperature gradient and debris characteristics uni-

form in the radial direction.

14. The effect of a wall (lower head) on the movement of the liquefied stainless steel is negligible.

In general, the assumptions are consistent with the expected behavior of the core plate and the expected characteristics of lower plenum debris. The omission of the inertial and capillary terms in the momentum equation is based on order of magnitude analyses; the results of these analyses are presented at the end of the section on numerical solution (Section 5), where results are calculated for representative cases.

Taking into account the above assumptions, the conservation of momentum equation for the liquefied material is given by the equation<sup>2,3</sup>

$$\frac{\mu_1 j}{k_1 k} + \frac{\rho_1 j^2}{m_1 m} = \rho_1 g \quad (2-1)$$

where

$\mu_1$	=	dynamic viscosity of liquefied material (kg/m · s),
$j$	=	superficial velocity of liquefied material (m/s),
$k$	=	Darcy permeability (m <sup>2</sup> ),
$k_1$	=	relative permeability (unitless),
$m$	=	passability of debris bed (m),
$m_1$	=	relative passability of debris bed (unitless),
$\rho_1$	=	density of liquefied material (kg/m <sup>3</sup> ),
$g$	=	acceleration of gravity (9.8 m/s <sup>2</sup> ).

The second term of the above equation is the turbulent drag counterpart to the viscous drag represented by the first term.

The Darcy permeability is calculated by the equation

$$k = \frac{\epsilon^3 D_p^2}{150(1 - \epsilon)^2} \quad (2-2)$$

where

$\varepsilon$  = porosity of the debris bed (unitless),

$D_p$  = diameter of particles in debris bed (m).

The passability of the debris bed is calculated by the equation

$$m = \frac{\varepsilon^3 D_p}{1.75(1 - \varepsilon)} \quad (2-3)$$

In general the relative passability is less than the relative permeability, but they are assumed to be equal for this analysis.<sup>4</sup> Thus,

$$m_l = k_l \quad (2-4)$$

The relative permeability is a function of the effective saturation of the debris bed and the Darcy permeability. The relative permeability is calculated by the equation<sup>2</sup>

$$\begin{aligned} k_l &= S_e^3, S_e > 0 \\ k_l &= 0, S_e \leq 0 \end{aligned} \quad (2-5)$$

where

$S_e$  = effective saturation of debris bed (unitless).

The effective saturation is calculated by the equation<sup>2</sup>

$$S_e = \frac{S - S_r}{1 - S_r} \quad (2-6)$$

where

$S_e$  = effective saturation of debris bed (unitless),

$S$  = true saturation of debris bed; volume fraction of liquefied material in pores of debris bed (unitless),

$S_r$  = residual saturation of debris bed (unitless).

The residual saturation,  $S_r$ , is a function of the surface tension of the liquid and of the degree of wetting of the solid material by the liquefied material. Reference 2 provides an empirical equation for calculating residual saturation that is appropriate for debris resulting from the disintegration of nuclear reactor cores. This equation is

$$S_r = \begin{cases} \frac{1}{86.3} \left[ \frac{\gamma \cos(\theta)}{k \rho_l g} \right]^{0.263} & ; 0 \leq \theta \leq 90^\circ \\ 0 & ; 90^\circ < \theta \leq 180^\circ \end{cases} \quad (2-7)$$

where

$\gamma$  = surface tension of the liquid (N/m),

$\theta$  = wetting contact angle (degrees).

In the case of liquefied material that does not wet the solid material ( $90^\circ < \theta < 180^\circ$ ), the residual saturation is equal to zero. An example of such a system is a debris bed composed of (U, Zr)O<sub>2</sub> and stainless steel.<sup>2</sup> In this case, bulk motion occurs at a relatively low values of bed saturation.

The conservation of mass equation is applied to obtain the relation of the rate of change with time of the local saturation of the debris bed to the local velocity of the liquefied debris and to the local rate of melting of the solid debris. The result is the equation

$$\frac{\partial S}{\partial t} = -\frac{1}{\varepsilon} \frac{\partial j}{\partial y} \quad (T_s < T_{sol}) \quad (2-8)$$

where

$t$  = time (s),

$y$  = spatial coordinate that defines elevation (defined in Figure 1-1)(m).

Equations (2-1) and (2-8) are a set of two equations for solving for the variables  $j$  and  $S$ . The terms  $k_l$  and  $m_l$  in Equation (2-1) are a function of  $S$  and thus contribute to the nonlinearity of the set of equations. Although the momentum equation in the model described in Reference 2 omits the turbulent term in Equation (2-1), a hand calculation for a possible debris bed condition indicated that for a saturated debris bed the omission of the turbulent term would result in a factor of three overprediction of the velocity of the liquefied material. These calculations are presented at the end of the section on the numerical solution (Section 5). So the turbulent term is being retained for the present model.

### 3. Effects of Material Movement on Debris Bed Heat Transfer

The movement of liquefied core plate material through the interstices in a porous debris bed results in the transport of energy within the debris bed. In addition, the movement of the liquefied material through the debris bed influences the thermal conductivity and heat capacity of the debris bed. As a result, the movement of liquefied material may have a significant influence on the temperature distribution within the debris bed. This section defines the change to be made to the heat transport equations in the COUPLE model<sup>1</sup> so as to account for the effect of material movement on temperature distribution.

The COUPLE model calculates the transport of heat through a porous medium by the equation

$$(\rho c_v)_e \frac{\partial T}{\partial t} = \frac{\partial}{\partial x} \left( K_e \frac{\partial T}{\partial x} \right) + \frac{\partial}{\partial y} \left( K_e \frac{\partial T}{\partial y} \right) + Q \quad (3-1)$$

where

$(\rho c_v)_e$	=	$(1 - \epsilon_h)(\rho c_v)_m$
$\rho$	=	density (kg/m <sup>3</sup> ),
$c_v$	=	constant volume specific heat (J/kg · K),
$K_e$	=	effective thermal conductivity (W/m · K),
$Q$	=	volumetric heat generation rate (W/m <sup>3</sup> ),
$T$	=	temperature of debris (K),
$\epsilon_h$	=	heat conduction porosity of debris ; $\epsilon(1 - S)$ (unitless),
$S$	=	saturation of debris bed,
$x$	=	spatial coordinate in horizontal direction (m),
$y$	=	spatial coordinate in vertical direction (m),
$m$	=	mixture of stainless steel and (U, Zr)O <sub>2</sub> .

The boundary conditions for equation (3-1) are defined by the code user. Boundary conditions are defined for the bottom and top surfaces, and left and right surfaces of the region being represented by the COUPLE model. The boundary conditions at these surfaces can be either adiabatic surface or convection and radiative heat transfer to fluid.<sup>1</sup> For the outer surface of a reactor vessel lower head submerged in water, the convective heat transfer is calculated using the Cheung model.<sup>5</sup> For other surfaces, the convective heat transfer is calculated by the RELAP5 convective heat transfer models.<sup>6</sup>

The above equation models heat transport through debris by conduction and radiation. To account for the transport of heat by the movement of liquefied material, the  $Q$  term in the above equation will be replaced by the term

$$Q_N = Q + Q_T \quad (3-2)$$

where

$$\begin{aligned} Q_N &= \text{net volumetric heat generation rate (W/m}^3\text{),} \\ Q_T &= \text{effective heat generation due to movement of liquefied material (W/m}^3\text{).} \end{aligned}$$

The variable  $Q_T$  in the above equation is a function of the rate of flow and internal energy of the liquefied material. The rate of flow of liquefied material into node  $n$  is calculated by the equation

$$M_F = 0.5(j_{n+1} + j_n)A\rho_1\Delta t \quad (3-3)$$

where

$$\begin{aligned} M_F &= \text{mass of liquefied material that flowed into node } n \text{ during time step (kg),} \\ j_{n+1} &= \text{superficial velocity of liquefied material at node } n+1 \text{ (m/s),} \\ A &= \text{average of cross sectional areas of nodes } n \text{ and } n+1 \text{ (m}^2\text{),} \\ \rho_1 &= \text{density of liquefied material flowing into node } n \text{ (kg/m}^3\text{),} \\ \Delta t &= \text{time step (s).} \end{aligned}$$

The above equation is formulated assuming that there is liquid material of only one type of composition, namely stainless steel.

The variable  $Q_T$  in Equation (3-2) at any node is then calculated by the equation

$$Q_{Tn} = M_F([u_l(T_F) - u_l(T_n)]/\Delta z_n\Delta t) \quad (3-4)$$

where

$$\begin{aligned} Q_{Tn} &= \text{effective heat generation due to movement of liquefied material at node } n \text{ (W/m}^3\text{),} \\ u_l(T_F) &= \text{internal energy of flowing liquefied material at its temperature of } T_F \text{ (J/kg)} \end{aligned}$$

(calculated by MATPRO function ZUNTH1),

$T_n$  = temperature of node n (K),

$A$  = cross sectional area ( $m^2$ ),

$\Delta z_n$  = height of node n (m).

The movement of liquefied material through the interstices of a porous debris bed influences the effective thermal conductivity of the debris bed.

The effective thermal conductivity is calculated by the equation

$$k_e = k_{ec} + k_r \quad (3-1)$$

where

$k_e$  = effective conductivity ( $W/m \cdot K$ ),

$k_{ec}$  = effective conductivity (conduction only) ( $W/m \cdot K$ ),

$k_r$  = radiative conductivity ( $W/m \cdot K$ ).

The Imura-Takegoshi<sup>7</sup> model for thermal conductivity is combined with the Vortmeyer<sup>8</sup> radiation model.

The Imura-Takegoshi model in equation form is given as follows:

$$k_{ec} = \left[ \Psi + \frac{1 - \Psi}{\phi + \frac{1 - \phi}{v}} \right] k_g \quad (3-2)$$

$$\phi = 0.3 \epsilon_h^{1.6} v^{-0.044} \quad (3-3)$$

$$v = \frac{k_s}{k_g} \quad (3-4)$$

$$\Psi = \frac{\epsilon_h - \phi}{1 - \phi} \quad (3-5)$$

where

- $k_g$  = thermal conductivity of vapor in pores ( $W/m \cdot K$ ),
- $k_s$  = thermal conductivity of mixture of stainless steel and  $(U, Zr)O_2$  ( $W/m \cdot K$ ),
- $\epsilon_h$  = porosity of debris for heat transfer calculations =  $\epsilon (1-S)$ .

The mixture thermal conductivity ( $k_s$ ) is calculated by the MATPRO function named ZUTCO1.<sup>9</sup>

The Vortmeyer model is given as

$$k_r = 4\eta\sigma D_p T^3 \quad (3-6)$$

where

- $\eta$  = radiation exchange factor (user-defined value, with default value of 0.8),
- $\sigma$  = Stefan-Boltzmann constant  $W/m^2 \cdot K^4$  ( $5.668 \times 10^{-8}$ ),
- $D_p$  = particle diameter (m),
- $T$  = temperature (K).

#### 4. Boundary Conditions for Case of Core Plate Melting Above Debris Bed

This section describes the boundary condition applied to the model for movement of liquefied core plate material through a ceramic porous debris bed below the core plate. Such a case is shown in Figure 4-1. For nodes at the top of the debris bed, the equation based on the principles of flow of liquefied material in a porous debris bed is replaced by an equation that defines the rate of melting of the core plate above the debris bed. In other words, Equation (3-3) in Section 3 is replaced by the equation

$$M_{FT} = AG\Delta t \quad (4-1)$$

where

- $M_{FT}$  = mass of liquefied material that flowed into a node at top of debris bed during time step (kg),
- $A$  = cross sectional area of the node ( $m^2$ ),
- $G$  = rate of melting of structure above debris bed per unit of cross sectional area ( $kg/s/m^2$ ),

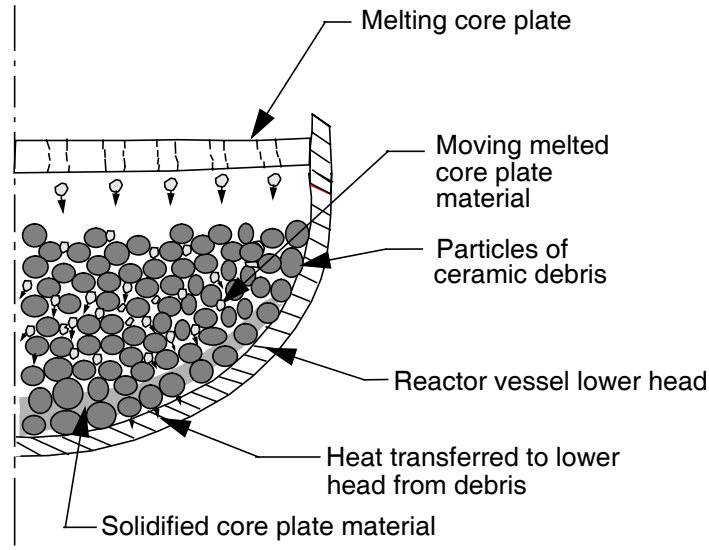


**Figure 4-1.** Schematic of material movement occurring when core plate melts and lower head supports ceramic porous debris.

$\Delta t$  = time step (s).

## 5. Numerical Solution

An explicit, iterative scheme for numerical solution is used to solve for the distribution in velocity and debris bed saturation. The scheme is based on the concept that the velocity gradient changes at a slower rate than the degree of bed saturation. In the first step for the first iteration, the change in bed saturation at each node is calculated using previous time step velocities in the neighborhood of each node. Next, the end of time step velocity at each node is calculated using the values for bed saturation calculated in the previous step. Next, the bed saturation at each node is calculated using the velocities just calculated for the end of the time step. If at any node the difference between the last two values calculated for bed saturation is greater than the tolerance for error in bed saturation, another iteration is performed. Subsequent iterations are performed until convergence is obtained at each node.

The equations in the numerical solution scheme are arranged as follows. First, a guess of the end of time step bed saturation is calculated using the equation

$$S_n^{m+1} = S_n^m - \frac{1}{\varepsilon} \left[ \frac{(j_{n+1}^m - j_{n-1}^m)}{(y_{n+1} - y_{n-1})} \right] \Delta t \quad (5-1)$$

where

$m$  = time step number,

$S_n^{m+1}$	=	bed saturation at node n at end of time step,
$S_n^m$	=	same as $S_n^{m+1}$ , but for start of time step,
$j_{n+1}^m$	=	superficial velocity at start of time step of liquefied material at node n+1 (m/s),
$j_n^m$	=	same as $j_{n+1}^m$ , but for node n (m/s),
$\varepsilon$	=	porosity for mass transport calculations (unitless),
$y_{n+1}$	=	elevation of node n+1 (m),
$y_n$	=	elevation of node n (m),
$\Delta t$	=	time step (s).

In the above equation, the nodes are assumed to have uniform cross sectional areas and uniform spacings in the vertical direction.

The moving of liquefied material changes the local porosity. Two categories of porosity need to be calculated at each node at each time step. One category of porosity, named the mass transport porosity, is used in the equations that calculate the flow of liquefied material. For this category, the volumes of liquid and gas are lumped together to represent the porosity. The other category of porosity, named the heat conduction porosity, is used in the equations that calculate the conduction of heat through the debris bed. For this category, the volumes of solid material and liquefied debris are lumped together.

The heat conduction porosity is related to the mass transport porosity by the equation

$$\varepsilon_h = \varepsilon(1 - S_n^{m+1}). \quad (5-2)$$

where

$\varepsilon_h$	=	heat conduction porosity (unitless),
$\varepsilon$	=	mass transport porosity (unitless),
$S_n^{m+1}$	=	saturation of debris bed (unitless).

Next, the Darcy permeability and the passability of the debris bed are updated using the equations

$$k_n = \frac{\varepsilon^3 D_p^2}{150(1 - \varepsilon)^2} \quad (5-3)$$

$$m_n = \frac{\varepsilon^3 D_p}{1.75(1 - \varepsilon)} \quad (5-4)$$

where

$k_n$  = Darcy permeability of debris bed at node n ( $m^2$ ),

$m_n$  = passability of debris bed at node n (m).

Next, the effective saturation of the debris bed at the end of the time step for each node is calculated using the equation

$$S_{en}^{m+1} = \frac{S_n^{m+1} - S_r}{1 - S_r} \quad (5-5)$$

where

$S_{en}^{m+1}$  = effective saturation at node n at end of time step.

The residual saturation,  $S_r$ , is a function of material properties, namely wetting angle, surface tension, Darcy permeability, and liquid density; it is calculated using Equation (2-7).

Next, the relative permeability of the debris bed at the end of the time step for each node is calculated using the equation

$$k_{ln}^{m+1} = [S_{en}^{m+1}]^3 \quad (5-6)$$

where

$k_{ln}^{m+1}$  = relative permeability at node n at end of time step,

The relative passability of the debris bed at the end of the time step for each node is calculated using the equation

$$m_{ln}^{m+1} = k_{ln}^{m+1} \quad (5-7)$$

where

$m_{ln}^{m+1}$  = relative passability of debris bed at node n at end of time step.

Next, the velocity of the liquefied material at each node is calculated using Equation (2-1). For numerical solution, terms in this equation are combined as follows

$$A[j_n^{m+1}]^2 + B j_n^{m+1} + C = 0 \quad (5-8)$$

where

$$\begin{aligned} A &= \frac{\rho_l}{m_{ln}^{m+1} m_n} \\ B &= \frac{\mu_l}{k_{ln}^{m+1} k_n} \\ C &= -\rho_l g \\ \rho_l &= \text{density of liquefied debris (kg/m}^3\text{)}, \\ \mu_l &= \text{dynamic viscosity of liquefied material kg/m} \cdot \text{s)}, \\ g &= \text{acceleration of gravity (9.8 m/s}^2\text{)}. \end{aligned}$$

Applying the quadratic equation, the superficial velocity of the liquefied material at each node at the end of the time step is calculated using the equation

$$j_n^{m+1} = \frac{-B \pm [B^2 - 4AC]^{0.5}}{2A} \quad (5-9)$$

The above equation has two values; since the liquefied material can only flow down, only the positive value is applied.

The bed saturation at each node at the end of the time step is then calculated using Equation (5-1) with the start of time step superficial velocities in this equation replaced with the end of time superficial velocities calculated by Equation (5-9).

The fractional difference in bed saturation between two successive iterations is calculated by the equation

$$f_n = \frac{|S_n^{i+1} - S_n^i|}{0.5(S_n^{i+1} + S_n^i)} \quad (5-10)$$

where

$$f_n = \text{fractional difference in value of } S_n^{m+1} \text{ between two successive iterations,}$$

$i$  = iteration number,

$S_n^i$  = value of  $S_n^{m+1}$  at  $i$ -th iteration.

If the value of  $f_n$  at any node is greater than the tolerance in error for bed saturation, another iteration is performed.

After convergence of the debris bed saturation at each node has been obtained, the effect of the movement of liquefied material during the time step on heat transport is calculated. First, the mass of material flowing into each node during the time step is calculated. For the top node in the debris bed, Equation (4-1) is used to calculate the mass of liquefied material that moved into this node during the time step. Then, Equation (3-4) is used to calculate the term added to the volumetric heat generation rate for each axial node to account for the transport of liquefied material. Then, the heat conduction porosity for each node is updated to account for the addition or subtraction of material from each node during the time step. Then, the atomic fractions of stainless steel and (U, Zr)O<sub>2</sub> at each node are updated to account for the addition or subtraction of material from each node during the time step. The particle size at each node is assumed to not be influenced by the presence of liquefied debris or frozen previously liquefied debris.

The mass of liquefied material added to or subtracted from each node is calculated by the equation

$$m_{an} = A\rho_l \left( j_{n+1}^{m+1} - j_{n-1}^{m+1} \right) \Delta t \quad (5-11)$$

where

$m_{an}$  = mass of liquefied material added to node  $n$  during time step (kg),

$A$  = cross sectional area of nodes (m<sup>2</sup>).

For the top node in the debris bed, the mass of liquefied material flowing into this node is calculated by the equation

$$m_{an} = AG\Delta t \quad (5-12)$$

where

$G$  = rate of melting of structure above the debris bed per unit of cross sectional area (kg/s)/m<sup>2</sup>.

To assure conservation of mass, the numerical solution is begun from the bottom most node and proceeds upward. At the bottom most node, the boundary condition of an impermeable boundary is imposed. Thus, the change in mass of stainless steel at this location is calculated by the equation

$$m_{a1} = 0.5A\rho_l(j_2^{m+1})\Delta t \quad (5-13)$$

The change in mass of stainless steel at other nodes is calculated using the mass added to the node below. Thus, the change in mass at axial node 2 is calculated by the equation

$$m_{a2} = (0.5A\rho_l(j_3^{m+1} + j_2^{m+1})\Delta t - m_{a1}) \quad (5-14)$$

Three constraints are applied to the motion of liquefied material. First, if the temperature at a location is less than the melting temperature of stainless steel, then that location is impermeable. Second, if liquid water is present at a location, then that location is impermeable. Third, if the temperature at any location is greater than the melting temperature of a mixture of  $UO_2$  and  $ZrO_2$ , then that location is impermeable. In general, if the condition for the second constraint is satisfied, then the condition for the first constraint is also satisfied. The third constraint is based on the assumption that melted (U, Zr) $O_2$  will flow a small distance, freeze, and form an impermeable crust. These constraints are applied by the equation

$$j_n^{m+1} = 0 \begin{cases} T_n < T_{ms} \\ T_n > T_{mu} \\ \alpha_f > 0 \end{cases}$$

where

$$\begin{aligned} T_{ms} &= \text{melting temperature of stainless steel (1671 K),} \\ T_{mu} &= \text{melting temperature of mixture of } UO_2 \text{ and } ZrO_2 \text{ (~3000 K),} \\ \alpha_f &= \text{volume fraction of liquid water.} \end{aligned}$$

If a crust of frozen (U, Zr) $O_2$  existed at a location before the melting of the core plate began, than that location is implicitly represented as impermeable from the assignment of a porosity of zero for that location.

Next, the calculation is made of the term to be added to the volumetric heat generation at each node to account for the thermal effect of the addition by flow of liquefied material to each node. This term is calculated by the equation

$$Q_{Tn} = m_{an}[u_l(T_F) - u_l(T_n)]/0.5(y_{n+1} - y_{n-1})A\Delta t \quad (5-15)$$

where

$$Q_{Tn} = \text{heat transported into node } n \text{ due to movement of liquefied material (W/m}^3\text{),}$$

$$\begin{aligned}
u_l(T_F) &= \text{internal energy of material flowing into node } n \text{ at temperature of } T_F \text{ (J/kg),} \\
T_F &= T_{n+1} \text{ (Temperature at node } n+1 \text{) for nodes other than top node; for top node,} \\
&\quad T_F = \text{temperature of material slumping onto top of debris bed (K),} \\
T_n &= \text{temperature of node } n \text{ (K).}
\end{aligned}$$

Next, the calculation is made of the atomic fractions of stainless steel and (U, Zr)O<sub>2</sub> at each node. The mass of stainless steel at each node at the end of a time step is calculated by the equation

$$m_{sn} = m_{sno} + m_{an} \quad (5-16)$$

where

$$\begin{aligned}
m_{sn} &= \text{mass of stainless steel at node } n \text{ at end of time step (kg),} \\
m_{sno} &= \text{mass of stainless steel at node } n \text{ at start of time step (kg).}
\end{aligned}$$

The atomic fractions are calculated by the equation

$$f_{sn} = \frac{m_{sn}}{a_{ws}} \left[ \frac{m_{sn}}{a_{ws}} + \frac{m_{un}}{a_{wu}} + \frac{m_{zn}}{a_{wz}} \right] \quad (5-17)$$

$$f_{zn} = \frac{m_{zn}}{a_{wz}} \left[ \frac{m_{sn}}{a_{ws}} + \frac{m_{un}}{a_{wu}} + \frac{m_{zn}}{a_{wz}} \right] \quad (5-18)$$

$$f_{un} = 1 - f_{sn} - f_{zn} \quad (5-19)$$

where

$$\begin{aligned}
f_{sn} &= \text{atomic fraction of stainless steel at node } n \text{ at end of time step,} \\
a_{ws} &= \text{atomic weight of stainless steel (56),} \\
m_{un} &= \text{mass of UO}_2 \text{ at axial node } n \text{ (kg),} \\
a_{wu} &= \text{atomic weight of UO}_2 \text{ (270),} \\
f_{un} &= \text{atomic fraction of UO}_2, \\
f_{zn} &= \text{atomic fraction of ZrO}_2
\end{aligned}$$

$m_{zn}$  = mass of  $ZrO_2$  at node n (kg),

$a_{wz}$  = atomic weight of  $ZrO_2$  (123.2).

In order to estimate the rate of movement of melted stainless steel through a medium of porous debris, Equation (5-8) was solved for two representative cases. In both cases, the debris and melted stainless steel are assumed to have the characteristics and properties<sup>4</sup> shown in Table 5-1. The solution was made for two values of effective saturation, namely  $S_e = 0.1$  and  $S_e = 1.0$ . The substitution of these values into the equations for the coefficients in Equation (5-8) gives the results shown in Table 5-2. The superficial velocities for the two values of effective saturation are shown in Table 5-3. The superficial velocities ranged from  $9.7 \times 10^{-5}$  m/s to  $2.9 \times 10^{-2}$  m/s. The table also shows the values calculated for superficial velocity when turbulent drag is neglected. For an effective saturation of 1.0, turbulent drag reduces the superficial velocity by a factor of three.

**Table 5-1.** Characteristics and properties for debris and melted stainless steel for scoping calculations.

Characteristic or property	Symbol	Units	Value
<i>porosity of debris</i>	$\epsilon$	-	0.4
<i>diameter of debris particles</i>	$D_p$	m	$2 \times 10^{-3}$
<i>density of liquefied stainless steel</i>	$\rho_l$	kg/m <sup>3</sup>	6920
<i>viscosity of liquefied stainless steel</i>	$\mu_l$	kg/m · s	$3.2 \times 10^{-3}$
<i>wetting angle of liquefied stainless steel in contact with (U, Zr)O<sub>2</sub></i>	$\theta$	degrees	120
<i>surface tension of liquefied stainless steel</i>	$\gamma$	N/m	0.45
<i>heat capacity of liquefied stainless steel</i>	$c_{pl}$	(J)/kg · K	690
<i>thermal conductivity at liquefied stainless steel</i>	$\lambda$	W/m · K	20

**Table 5-2.** Values of coefficients in Equation (5-8) for two representative cases.

Effective saturation	A	B	C
0.1	$5.67 \times 10^{10}$	$6.77 \times 10^8$	$-6.78 \times 10^4$
1.0	$5.67 \times 10^7$	$6.77 \times 10^5$	$-6.78 \times 10^4$

**Table 5-3.** Superficial velocities for two representative cases.

Effective saturation	Superficial velocity(m/s)	
	Turbulent drag	No turbulent drag
<i>0.1</i>	$9.7 \times 10^{-5}$	$1.0 \times 10^{-4}$
<i>1.0</i>	$2.9 \times 10^{-2}$	<i>0.10</i>

The relatively slow movement of the liquefied stainless steel allows the inertial terms to be neglected in the momentum equation without significant loss of accuracy. For the case of saturated debris, which results in an upper bound on the velocity of the liquefied stainless steel, the gravity and viscous terms in the momentum equation are of order of  $5 \times 10^4 \text{ N/m}^3$ , while the inertial terms<sup>3</sup> are estimated to be of order of  $1 \times 10^3 \text{ N/m}^3$ .

Inclusion in the the calculations of capillary forces would not significantly change the velocities shown in Table 5-3. The capillary forces are a function of the porosity and particle size of the debris, surface tension of the liquid stainless steel, and the wetting angle of liquefied stainless steel in contact with (U, Zr)O<sub>2</sub>.<sup>2,3</sup> The values of the latter two properties are not firmly established.<sup>2</sup> Assuming values for these latter two properties that result in an upper bound on the capillary forces, and assuming a gradient in effective saturation of 10.0/m, the capillary force term in the momentum equation is estimated to be of order of  $0.7 \times 10^4 \text{ N/m}^2$ , which is an order of magnitude smaller than the gravitational and viscous terms.

The relatively slow movement of the liquefied stainless steel justifies the assumption of thermal equilibrium between the stainless steel and the (U, Zr)O<sub>2</sub>. The time constant for conduction heat transfer to the stainless steel in the interstices of the porous debris is approximated by the equation

$$\tau = \frac{\rho_1 c_{pl} (\Delta x)^2}{6\lambda} \quad (5-20)$$

where

$\tau$  = time constant (s),

$\rho_1$  = density of liquefied stainless steel ( $6920 \text{ kg/m}^3$ ),

$c_{pl}$  = heat capacity of liquefied stainless steel ( $690 \text{ J/kg} \cdot \text{K}$ ),

$\Delta x$  = average thickness of interstices, which is estimated to be approximately equal to the diameter of the UO<sub>2</sub> particles ( $2 \times 10^{-3} \text{ m}$ ),

$\lambda$  = thermal conductivity of liquefied stainless steel ( $20 \text{ W/m} \cdot \text{k}$ ).

The time constant for conduction heat transfer is calculated to be 0.16 s. Assuming a maximum temperature gradient in the (U, Zr)O<sub>2</sub> of 1000 K/m, the liquefied stainless steel needs to flow for 34 s

before experiencing a factor to two change in its ambient temperature. This order of magnitude larger time than the time constant for conduction heat transfer indicates that the assumption of thermal equilibrium of the stainless steel and (U, Zr)O<sub>2</sub> is justified.

## 6. Implementation into COUPLE model

This section identifies the extensions made to the data base of the COUPLE model and to its subroutines in order to implement the numerical solution for the movement of liquefied core plate material through a porous debris bed. The variables added to the COUPLE model data base are described in Table 6-1. This table also defines the Fortran name assigned each variable added to the COUPLE data base and identifies its corresponding name in the numerical solution section of this report. The table also identifies the subroutines that calculate the values of the new variables. The arrays in Table 6-1 are stored in the COUPLE bulk storage array named “a,” which is stored in the common block named “alcm.” The pointers in Table 6-1 are stored in the COUPLE common block named “iparm.” In order to improve computational efficiency, several variables in the numerical solution are omitted from Table 6-1, such as (1) density of liquid material, and (2) dynamic viscosity of liquid material. These variables are stored as local variables in the subroutines that use them.

**Table 6-1.** Variables added to COUPLE data base for modeling of flow of liquefied material within porous debris bed .

variable definition	Fortran name	Numerical solution name	units	subroutines that calculate variable
<i>pointer to variable storing bed saturation at current iteration at element n</i>	<i>iptbst</i>	-	-	<i>AUMESH</i>
<i>bed saturation at element n at current iteration</i>	<i>a(iptbst+n-1)</i>	$S_n^m + I$	-	<i>MOV CPL</i>
<i>pointer to variable storing bed saturation at previous iteration</i>	<i>iptbs0</i>	-	-	<i>AUMESH</i>
<i>bed saturation at element n at previous iteration</i>	<i>a(iptbs0+n-1)</i>	$S_n^m$	-	<i>MOV CPL</i>
<i>pointer to variable storing effective bed saturation at element n</i>	<i>iptebs</i>	-	-	<i>AUMESH</i>
<i>effective bed saturation at element n</i>	<i>a(iptebs+n-1)</i>	$S_{en}$	-	<i>MOV CPL</i>
<i>pointer to array storing Darcy permeability at element n</i>	<i>iptprm</i>	-	-	<i>AUMESH</i>
<i>Darcy permeability at element n</i>	<i>a(iptprm+n-1)</i>	$k_n$	$m^2$	<i>MOV CPL</i>
<i>pointer to array storing passability at element n</i>	<i>iptpas</i>	-	-	<i>AUMESH</i>

**Table 6-1.** Variables added to COUPLE data base for modeling of flow of liquefied material within porous debris bed (continued).

variable definition	Fortran name	Numerical solution name	units	subroutines that calculate variable
<i>passability at element n</i>	<i>a(iptpas+n-1)</i>	$m_n$	<i>m</i>	<i>MOVCPL</i>
<i>pointer to variable storing relative permeability at element n</i>	<i>iptrpr</i>	-	-	<i>AUMESH</i>
<i>relative permeability at element n</i>	<i>a(iptrpr+n-1)</i>	$k_{ln}$	-	<i>MOVCPL</i>
<i>pointer to array storing mass of stainless steel in element n</i>	<i>iptmss</i>	-	-	<i>AUMESH</i>
<i>mass of stainless steel in element n</i>	<i>a(iptmss+n-1)</i>	-	<i>kg</i>	<i>MUPDAT, MOVCPL</i>
<i>pointer to array storing mass of (U, Zr)O<sub>2</sub> in element n</i>	<i>iptmuo</i>	-	-	<i>AUMESH</i>
<i>mass of (U, Zr)O<sub>2</sub> in element n</i>	<i>a(iptmuo+n-1)</i>	-	<i>kg</i>	<i>MUPDAT, MOVCPL</i>
<i>pointer to array storing superficial velocity of liquefied material after current iteration at node n</i>	<i>iptjlm</i>	-	-	<i>AUMESH</i>
<i>superficial velocity of liquefied material at end of current time step at node n</i>	<i>a(iptjlm+n-1)</i>	$j_n^{m+1}$	<i>m/s</i>	<i>MUPDAT, MOVCPL</i>
<i>pointer to array storing superficial velocity of liquefied material after previous iteration at node n</i>	<i>iptjl0</i>	-	-	<i>AUMESH</i>
<i>superficial velocity of liquefied material at start of current time step at node n</i>	<i>a(iptjl0+n-1)</i>	$j_n^m$	<i>m/s</i>	<i>MOVCPL</i>

Several user-defined variables are required for the numerical solution; these variables are identified in Table 6-2. Two of the variables in Table 6-2 are material properties that are not defined in the material properties part (MATPRO)<sup>9</sup> of SCDAP/RELAP5. These variables are the liquid-solid contact angle and the surface tension of liquefied stainless steel. When the values of these material properties are firmly established, the values will be obtained from MATPRO instead of being user-defined. Another variable in this table, namely the rate of melting of the core plate above a debris bed can be obtained from calculations performed by the core plate model in SCDAP/RELAP5. Nevertheless, it is useful to make this variable

user-defined for testing and for analyses focusing on behavior of debris in the lower head of a reactor vessel instead of on behavior of an overall reactor system.

**Table 6-2.** User-defined variables added to data base for modeling of flow of liquefied material within porous debris bed .

Variable definition	Fortran name	Numerical solution or theory name	Units	Common block
<i>liquid-solid contact angle (wetting angle)</i>	<i>thtwet</i>	$\theta$	<i>radians</i>	<i>tblsp</i>
<i>surface tension of liquefied material</i>	<i>gamwet</i>	$\gamma$	<i>N/m</i>	<i>tblsp</i>
<i>rate of slumping of melting structure located directly above debris bed</i>	<i>mdtstr</i>	$G$	<i>(kg/s)/m<sup>2</sup></i>	<i>tblsp</i>
<i>accuracy of calculated bed saturation</i>	<i>accbst</i>	-	-	<i>tblsp</i>

The model for calculating the movement of liquefied stainless steel was programmed in a new subroutine named MOVCP. This new subroutine is called from subroutine COUPLE just before the call to subroutine EGEN2. The new subroutine calculates the distribution of liquefied stainless steel within the debris bed and calculates the addition or subtraction to be made to the volumetric heat generation term in the COUPLE model in order to account for the transport of heat by movement of liquefied material. The new subroutine also calculates the change in effective thermal conductivity and heat capacity at each node due to movement of liquefied material. The Fortran programming of the new subroutine is based on the numerical solution scheme outlined in Section 5 of this report.

The extensions made to existing COUPLE subroutines are summarized in Table 6-3. Subroutine MATERL was extended to define input needed for the models that calculate the movement of liquefied material. Subroutine AUMESH was extended to reserve storage for the new variables added to the COUPLE model to calculate the movement of liquefied material and its consequences. Subroutine ICPL was extended to initialize the new variables added to the COUPLE model. Subroutine COUPLE was extended to call the new subroutine named MOVCP, which calculates the movement of liquefied material and its consequences. Subroutine MAJCOU was extended to display the results calculated by subroutine MOVCP.

**Table 6-3.** Extensions to existing COUPLE subroutines for modeling flow of liquefied material within porous debris bed .

Subroutine	Line in subroutine	Extensions
<i>MATERL</i>	<i>read(eoin,1005)emissm</i>	<i>add to this read statement the definition of input variables listed in Table (6-3)</i>

**Table 6-3.** Extensions to existing COUPLE subroutines for modeling flow of liquefied material within porous debris bed (continued).

Subroutine	Line in subroutine	Extensions
<i>AUMESH</i>	<i>i111=i110+4*numel</i>	<i>after this line, define pointers listed in Table (6-2) and reserve storage for variables associated with the pointers</i>
<i>ICPL</i>	<i>do 50 i=1,numel</i>	<i>in this do loop, initialize to value of zero the variables in Table (6-2) with element number for index</i>
<i>COUPLE</i>	<i>call egen2(a(i8),....</i>	<i>before this line, add call to new subroutine named MOVCPPL to obtain movement of liquefied material and its consequences</i>
<i>MAJCOU</i>	<i>1575 format(... end if</i>	<i>after these lines, print values of bed saturation and porosity in each element and velocity of liquefied stainless steel</i>

## 7. Testing and Assessment of Implemented Models

The models added to SCDAP/RELAP5 will be tested and assessed using two test problems. The matrix of test problems is described in Table 7-1.

**Table 7-1.** Matrix of test problems for assessing models of liquefied material moving through porous debris bed .

Problem no.	Problem description	Focus of assessment
<i>1</i>	<i>Liquefied stainless steel slumps onto top of hot porous debris bed composed of (U, Zr)O<sub>2</sub> and then flows through the debris bed</i>	<i>Internal consistency of modeling, including maintaining of conservation of mass and energy</i>
<i>2</i>	<i>Except for porosity and particle size, same as Problem No. 1</i>	<i>Evaluate sensitivity of results to debris characteristics, rate of melting of core plate and convergence criterion</i>

The first problem involves the calculation of the flow of liquefied stainless steel that slumps onto the top of a porous debris bed. The test problem is described in Figure 7-1. The debris bed has an initial

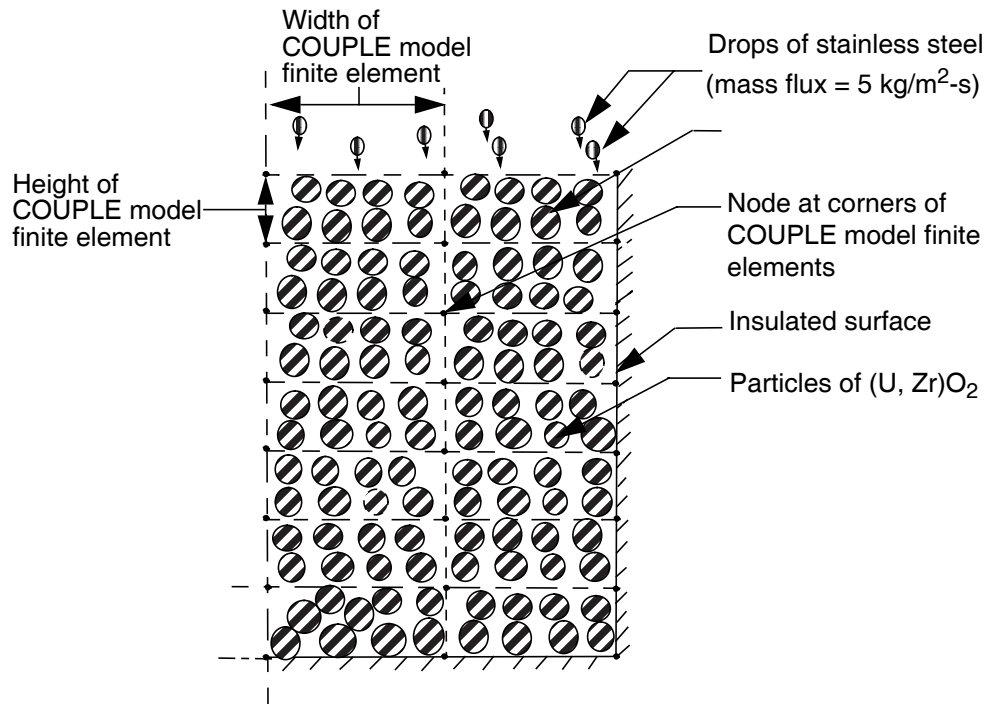


**Figure 7-1.** Description of Test Problem Number 1.

temperature of 2500 K and the slumping liquefied stainless steel has a temperature of 1700 K just before contact with the top surface of the debris bed. The debris particles have a volumetric heat generation rate of 1 MW/m<sup>3</sup>. The debris particles are composed of (U, Zr)O<sub>2</sub> with a diameter of 2 mm. The initial porosity of the debris bed is 0.5. No water or steam is flowing through the debris bed. The debris is represented by two parallel stacks of COUPLE model finite elements, with twenty elements in each stack.

The second problem evaluates the sensitivity of calculated results to debris characteristics, rate of melting of the core plate, and convergence criterion.

## 8. Summary

Designs were described for models to calculate the movement of liquefied core plate through the interstices of porous debris composed of (U, Zr)O<sub>2</sub> particles. The models are intended for implementation into the COUPLE model in SCDAP/RELAP5 so as to give it the capability to calculate the effect on lower head heatup of liquefied core plate material moving through porous debris in the lower head. Equations and solution methods were presented for the calculation of the motion of liquefied and the heat transported by the moving material. The liquefied material is calculated to move until either it freezes, reaches a location in the debris bed where the degree of bed saturation is less than the residual saturation, or reaches an impermeable boundary. Equations were also presented for calculating the effect of moving material on effective thermal conductivity and heat capacity. A description was presented of the extensions in COUPLE model Fortran programming required to implement these equations and solution methods. A matrix of test problems was defined for assessing these models and their implementation.

## 9. References

1. The SCDAP/RELAP5 Development Team, "SCDAP/RELAP5/MOD3.2 Code Manual, Volume 2: Damage Progression Model Theory," NUREG/CR-6150, Volume 2, Rev. 1, INEL-96/0422, July 1998.
2. R. C. Schmidt and R. D. Gasser, "Models and Correlations of the DEBRIS Late-Phase Melt Progression Model," SAND93-3922, September 1997.
3. L. J. Siefken, "SCDAP/RELAP5 Modeling of Movement of Melted Material Through Porous Debris in Lower Head," INEEL/EXT-98-01178, December 1998.
4. Mo Chung and Ivan Catton, "Post-Dryout Heat Transfer in a Multi-Dimensional Porous Bed," Nuclear Engineering and Design 128 (1991) pages 289-304.
5. F. B. Cheung, K. H. Hadded, and Y. C. Liu, "A Scaling Law for the Local CHF on the External Bottom Side of a Fully Submerged Reactor Vessel," NUREG/CP-0157, Vol. 2, February 1997, pp. 253-277.
6. The RELAP5 Development Team, "RELAP5 Code Manual, Models and Correlations," NUREG/CR-5535, Vol. 4, August 1995.
7. S. Imura and E. Takegoski, "Effect of Gas Pressure on the Effective Thermal Conductivity of Packed Beds," Heat Transfer Japanese Research, 3, 4, 1974, p. 13.
8. D. Vortmeyer, "Radiation in Packed Solids," 6th International Heat Transfer Conference, Toronto, Canada, 1978.
9. The SCDAP/RELAP5 Development Team, "SCDAP/RELAP5/MOD3.2 Code Manual, Volume 4: MATPRO - A Library of Materials Properties for Light-Water-Reactor Accident Analysis," NUREG/CR-6150, Volume 4, Rev. 1, INEL-96/0422, July 1998

